Supporting Information for

"Small Polarons in Two-Dimensional Pnictogens: A First-Principles Study"

Vasilii Vasilchenko,[†] Sergey Levchenko,[†] Vasili Perebeinos,[‡] Andriy Zhugayevych[†]

[†] *Skolkovo Institute of Science and Technology, Moscow 143026, Russia*
[‡] *Department of Electrical Engineering, University at Buffalo, NY 14260, USA*

E-mail: a.zhugayevych@skoltech.ru

May 11, 2021

S1 Considered clusters S2
S2 Size convergence of calculations of undistorted clusters S4
S3 Benchmarking basis sets S8
S4 Benchmarking density functionals against CCSD S10
S5 Benchmarking density functionals by Koopman's theorem S13
S6 Main parameters of blue- and black-P monolayers S14
S7 Electronic structure of monolayers S17
S8 Polaron wave-function and lattice deformation S23
S9 Size convergence studies of hole polaron in blue-P S28
S10 Potential energy surfaces S33
S11 Excited states S38
S12 Triplet exciton S39
S13 Results for arsenic S41
S14 Results for antimony S44
S15 Atomic data for pnictogens and related elements S46
S16 Dependence on cluster passivation S47

S1 Considered clusters

Table S1: Considered series of clusters. Some small blue and black clusters corresponding to $n = 1$ are identical: `rlayer1`=`olayer1`=`cluster1`, `rlayer2`=`olayer2`=`cluster2`.

Centering	Series ($n \in \mathbb{N}$)	List of considered N	blue symmetry	black symmetry
atom	$N = 6n(n-1)+1$	1, 13, 37, 73, 121, 181	3m	m
bond	$N = 2n(3n-2)$	2, 16, 42, 80, 130, 192	2/m	2/m
ring	$N = 6n^2$	6, 24, 54, 96, 150	-3m	2/m

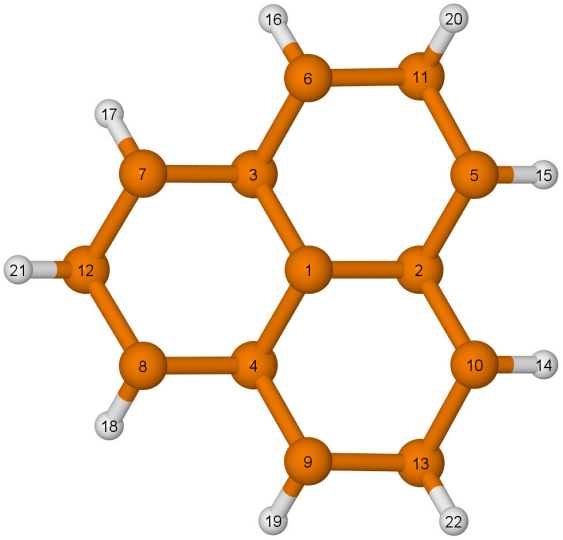

(a) `rlayer13` ($N = 13$)

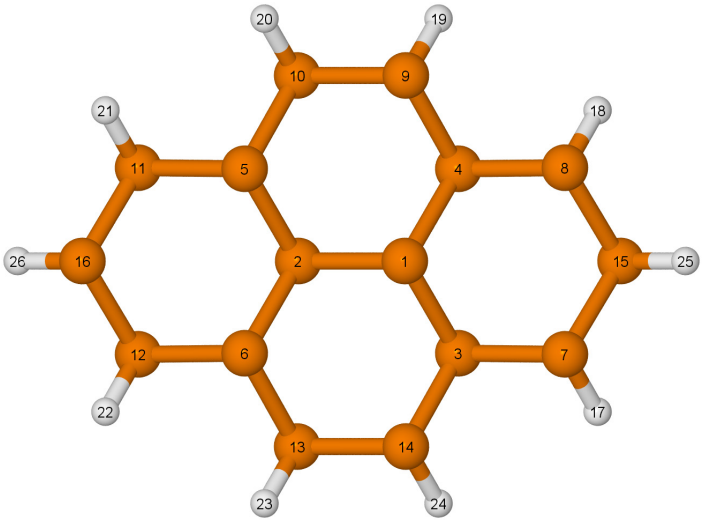

(b) `rlayer16` ($N = 16$)

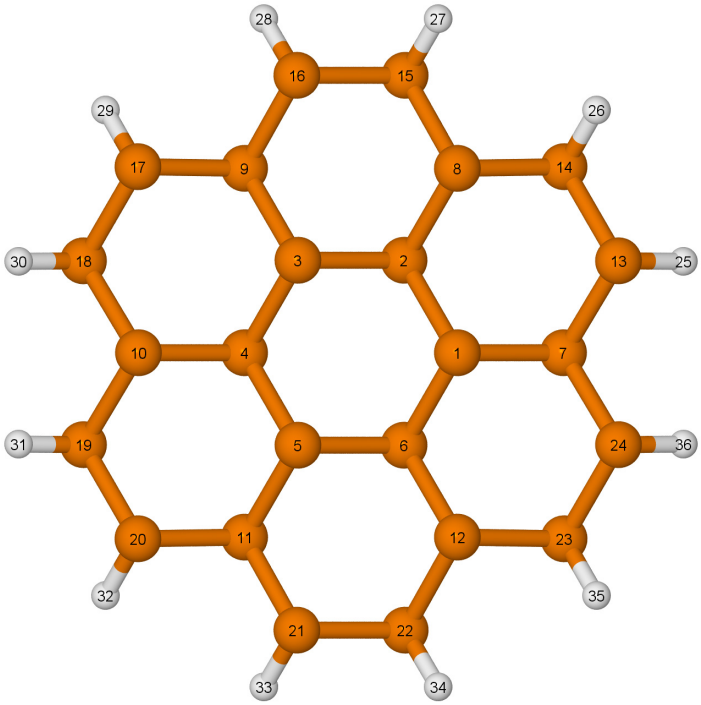

(c) `rlayer24` ($N = 24$)

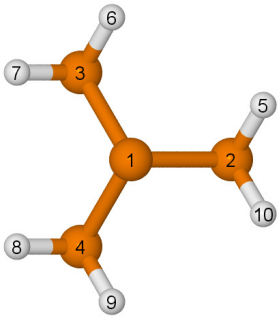

(d) `cluster4` ($N = 4$)

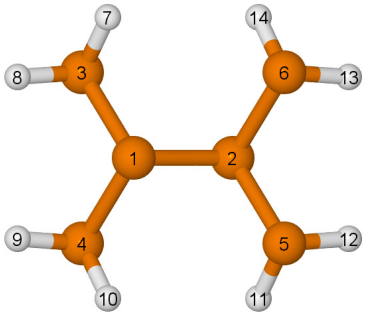

(e) `cluster6` ($N = 6$)

Figure S1: Considered clusters: (a-c) representative serial blue clusters corresponding to $n = 2$; (d-e) small non-serial clusters.

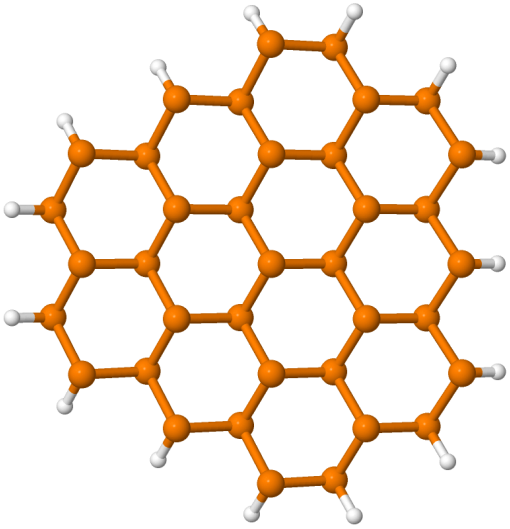

(a) `rlayer37`

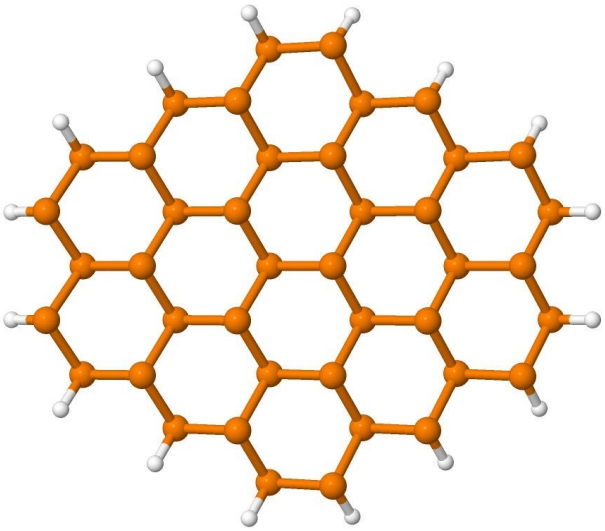

(b) `rlayer42`

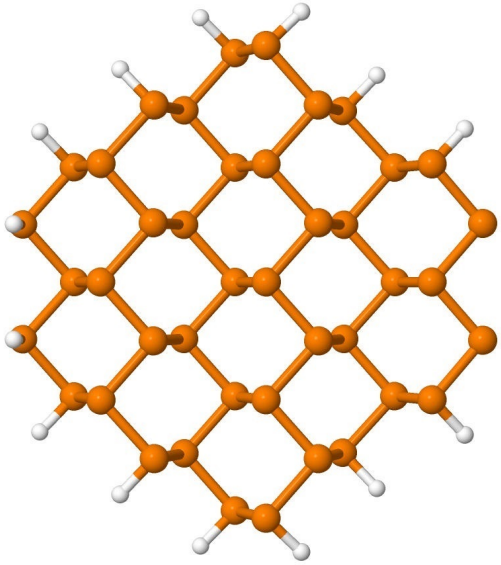

(c) `olayer42`

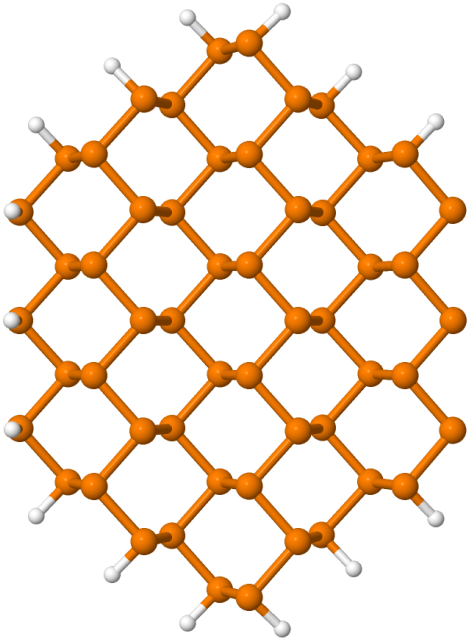

(d) `olayer54`

Figure S2: Other examples of serial clusters. Blue and black allotropes are distinguished by prefix 'r' and 'o' meaning rhombohedral and orthorhombic three-dimensional crystal systems.

S2 Size convergence of calculations of undistorted clusters

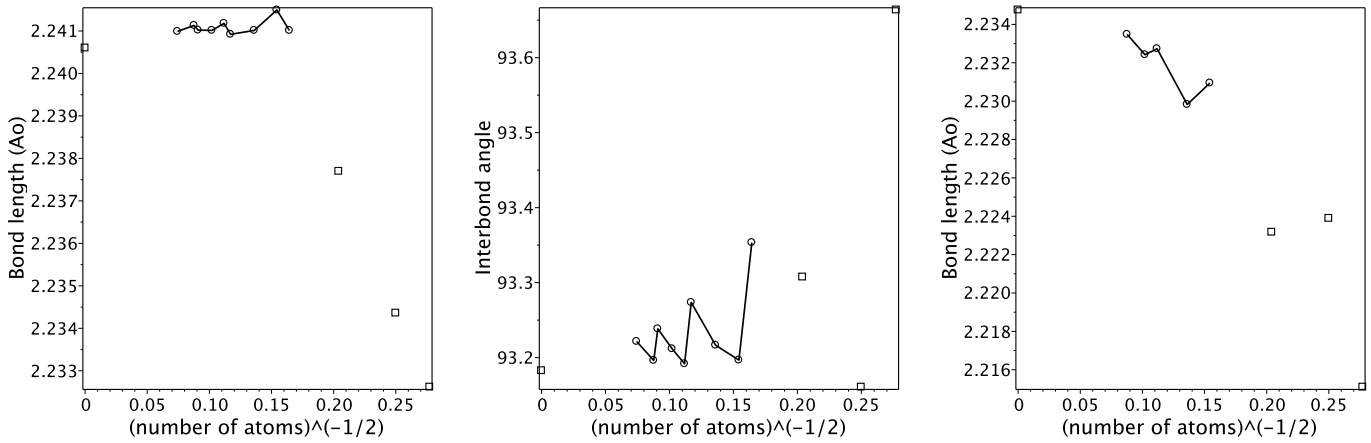

(a) Blue-P (b) Blue-P (c) Black-P

Figure S3: Convergence of local geometry is fast: no extrapolation is needed because a central region of even small clusters have geometry of the infinite cluster. Values at zero are calculated for translationally invariant system.

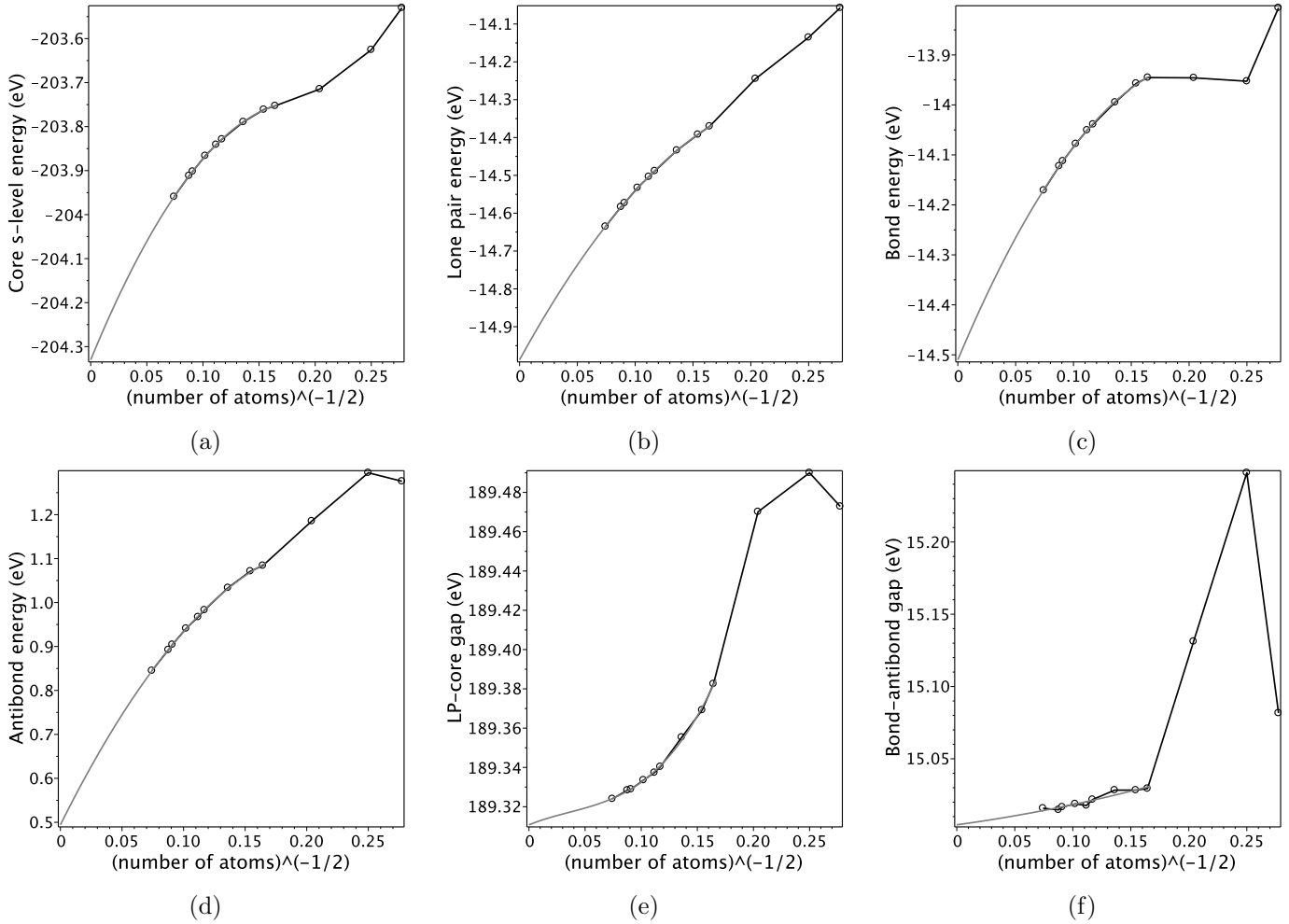

(a) (b) (c)

(d) (e) (f)

Figure S4: Convergence of NBO energies for blue-P: (a-d) absolute energies converge slowly, (e-f) relative energies converge quickly.

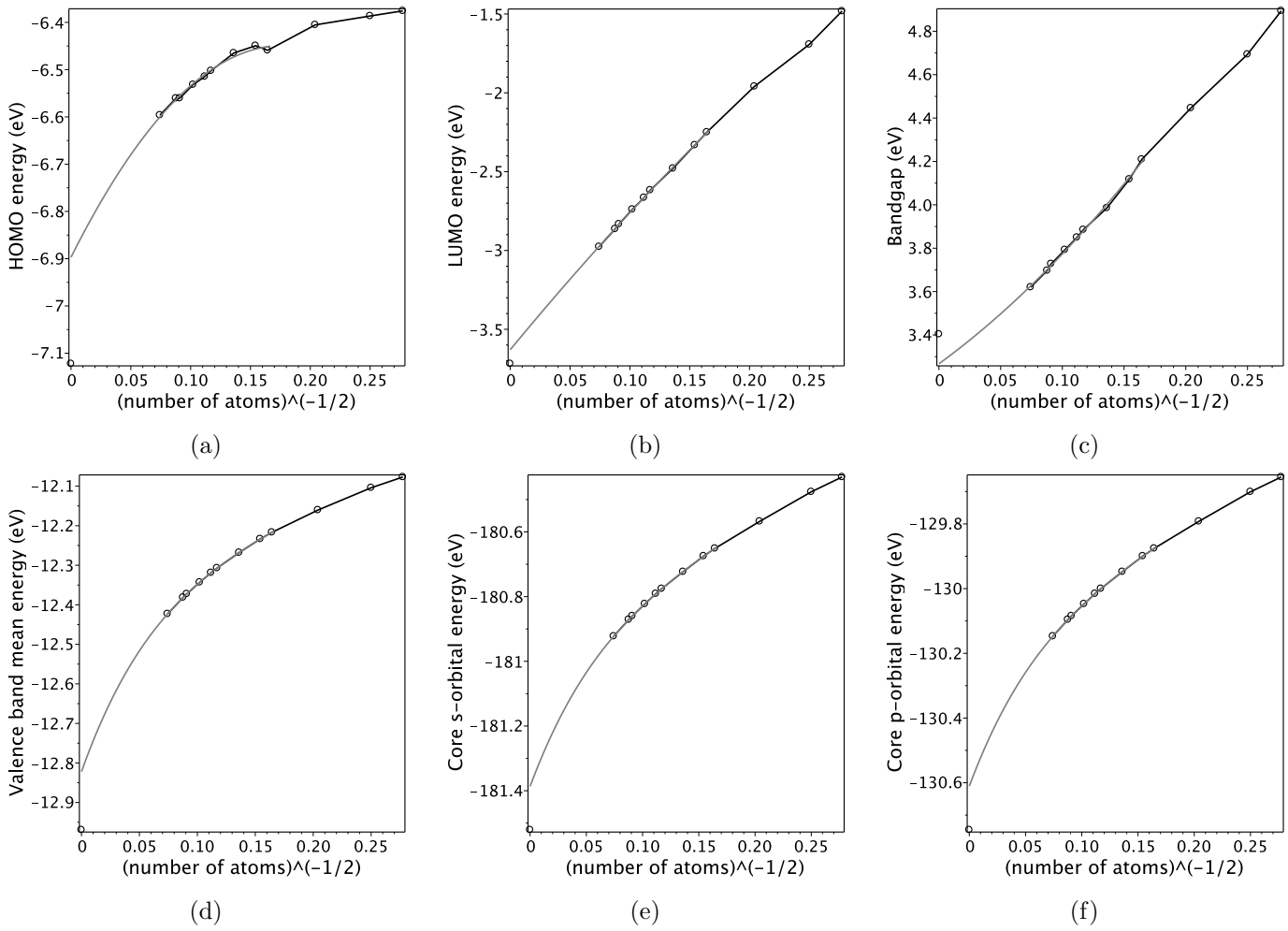

Figure S5: Convergence of MO energies is slow especially for HOMO: larger clusters are required to converge to 0.1 eV precision (see follow-up figures for explanation). For panels (d-f) the size dependence is smoother, so that 4th order polynomial fit (in $N^{-1/2}$) allows to get that precision. Data for blue-P are shown here.

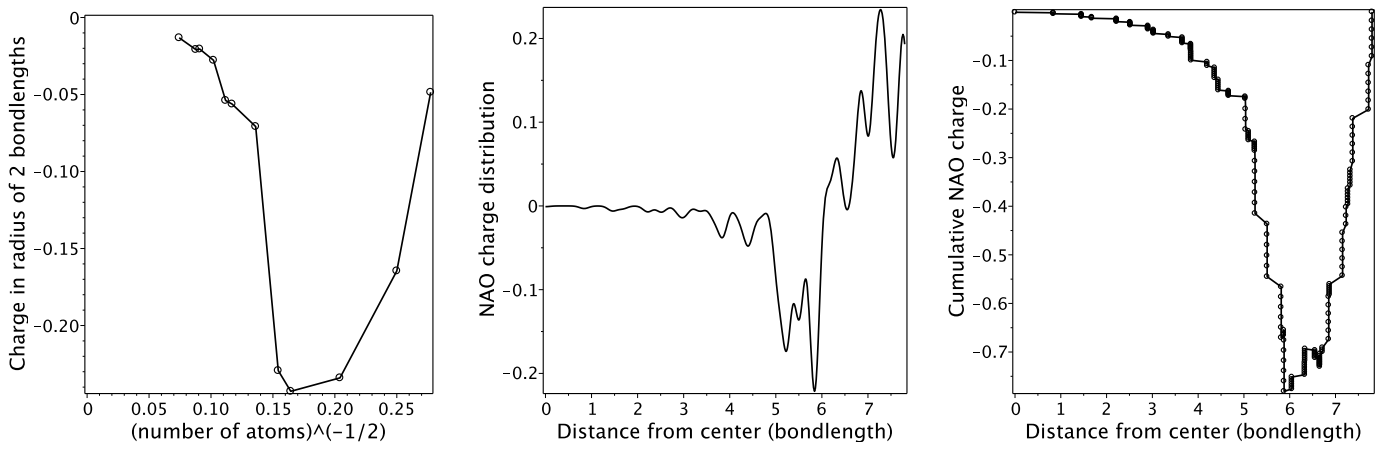

(a) Convergence of the total charge within 2 bondlengths from cluster center (12-14 atoms depending on cluster symmetry).

(b) Radial charge distribution for 181-atom cluster.

(c) Cumulative radial charge distribution for 181-atom cluster.

Figure S6: Natural atomic orbital (NAO) charges for blue-P. The surface layer has the width of 2-4 pnictogens, therefore only for clusters with 50-100 atoms the central region has no artificial extra charge.

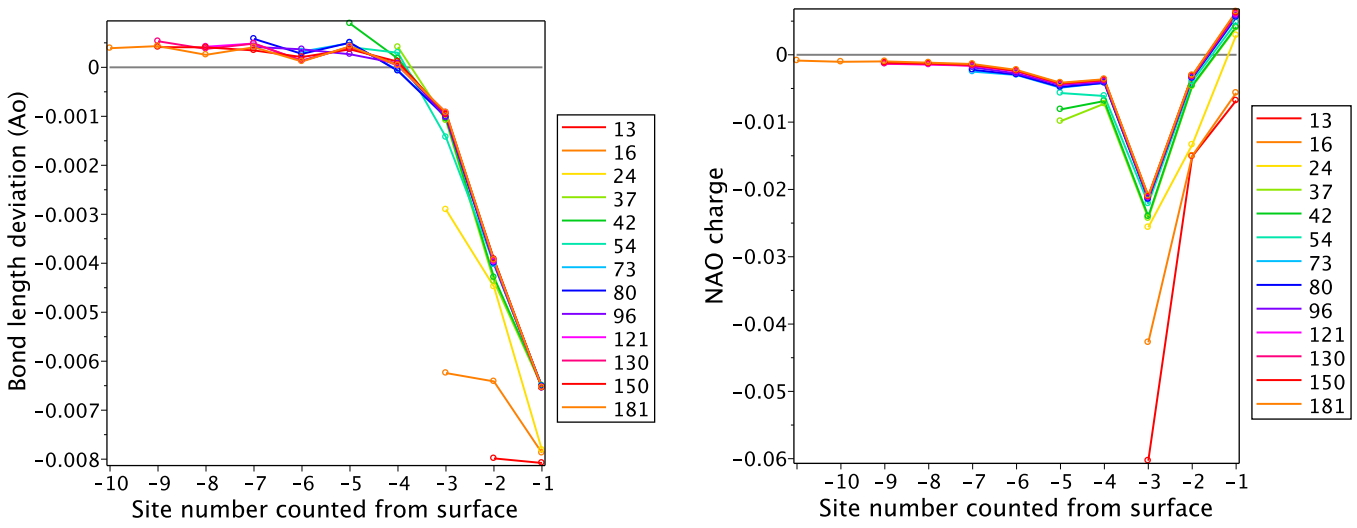

(a) (b)

Figure S7: Radial distribution of (a) bond lengths and (b) NAO atomic charges for blue-P.

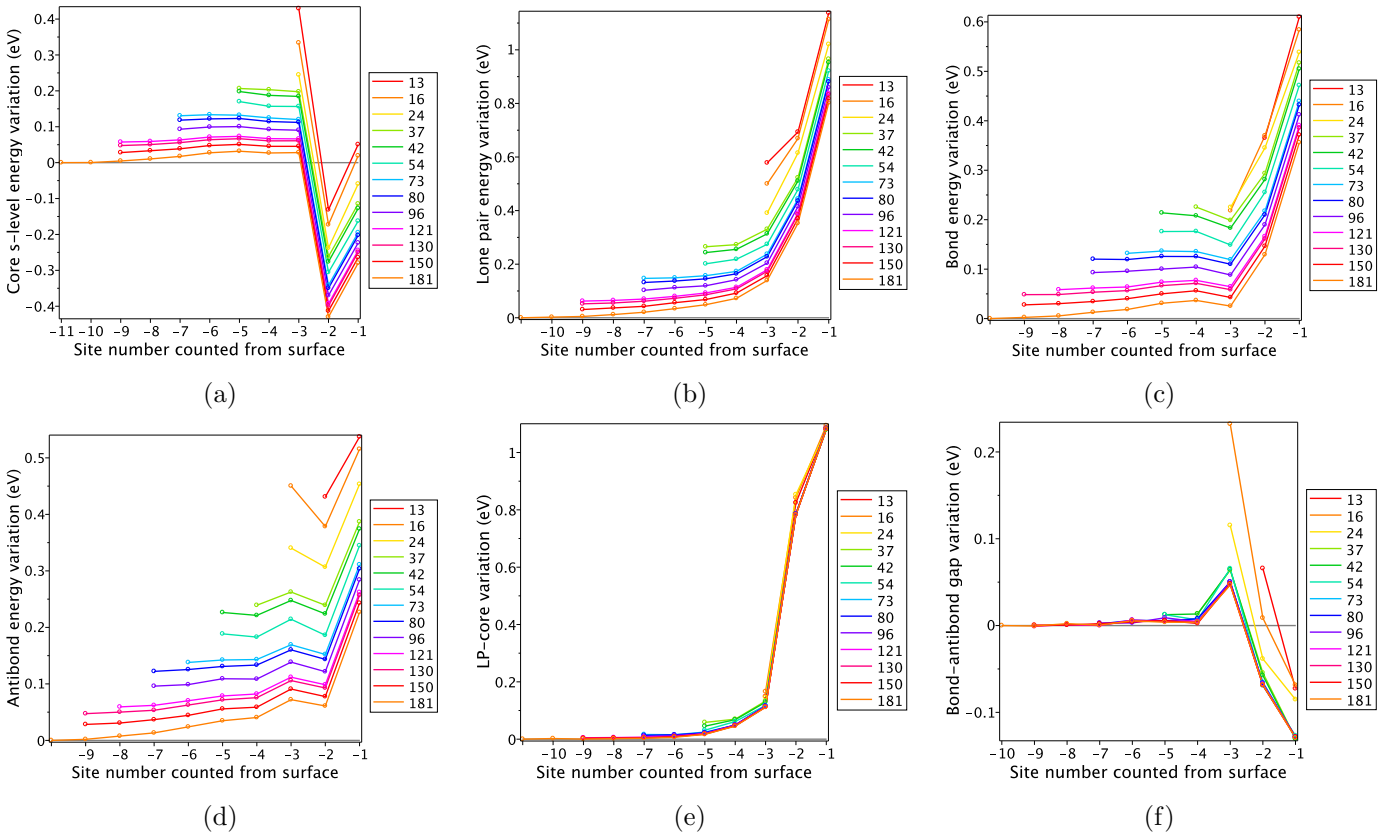

(a) (b) (c)

(d) (e) (f)

Figure S8: Radial distribution of various NBO energies for blue-P: (a-d) absolute energies converge slow, but (e-f) relative energies converge quickly in the central region.

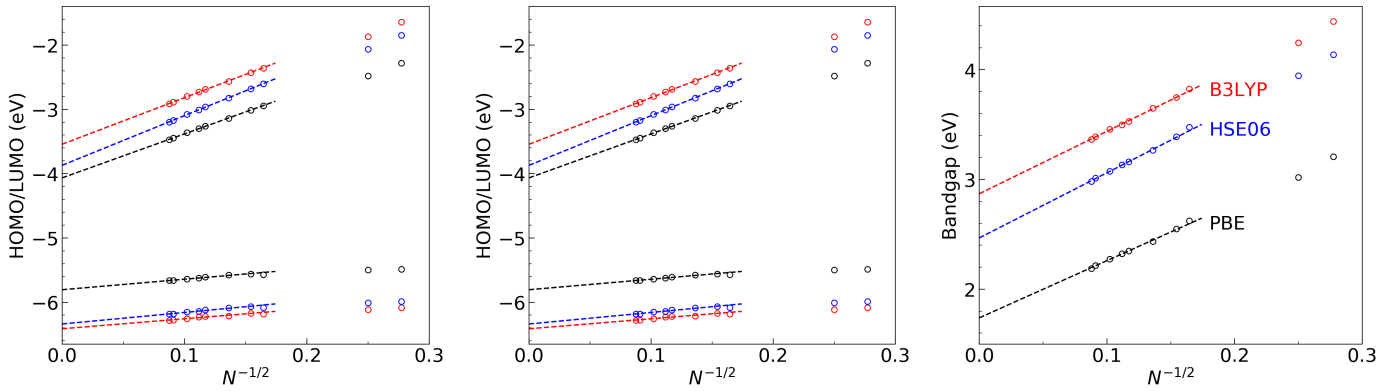

(a) (b) (c)

Figure S9: Convergence of cluster calculations for blue-P for other considered density functionals. N denotes number of pnictogen atoms in a cluster. Dashed lines extrapolate the values to the limit of an infinite-size cluster. Note that at the scale of methods comparison, the above mentioned slow size convergence effects are negligible.

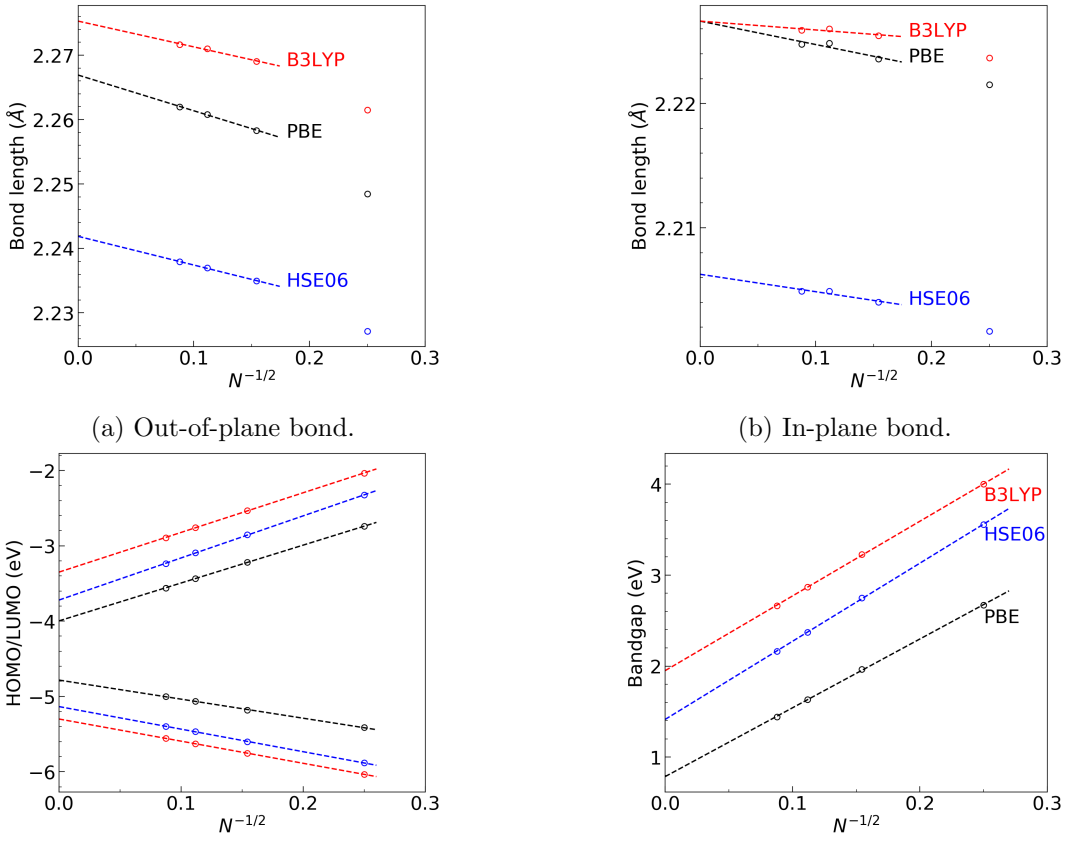

(a) Out-of-plane bond.

(b) In-plane bond.

(c)

(d)

Figure S10: Convergence of cluster calculations for black-P for other considered density functionals.

S3 Benchmarking basis sets

Basis sets are tested for As clusters using B3LYP functional. Basis set abbreviations: 'anp' – Ahlrichs basis sets with n valence orbitals, 'cn' – Dunning basis sets, 'a' means diffuse orbitals, 'p2p'=6-31G*. Cluster abbreviations: C=cluster, L=rlayer, oL=olayer, R6 and oR6 are hydrogen-passivated rings in blue and black layers, P/N means cation/anion. Rows are ordered by 'C6' column. Evidently, 6-31G* basis fails for arsenic.

Bond length (Angstroms)

basis	C1	C2	C4	C6	C6_P	C6_N	R6	oR6	L13	L13_P	L16	L16_N	oL16
a4p	1.524	2.488	2.496	2.501	2.438	3.121	2.497	2.485	2.501	2.463	2.503	3.215	2.496
p2p	0.019	-0.033	-0.040	-0.049	-0.050	-0.257	-0.043	-0.054	-0.054	-0.050	-0.054	-0.760	-0.088
c4a	-0.001	-0.000	-0.000	-0.000	-0.000	-0.014	-0.000	-0.000	-0.000	-0.000	-0.000	-0.007	-0.000
c4	-0.000	0.000	0.000	0.000	0.000	0.001	0.000	0.000	0.000	0.000	0.000	0.001	0.000
a3p	0.002	-0.000	0.001	0.001	0.000	0.012	0.000	-0.001	0.001	0.001	0.001	0.006	-0.001
c3a	0.001	0.002	0.002	0.002	0.002	-0.010	0.002	0.002	0.002	0.002	0.002	-0.005	0.002
c3	0.001	0.002	0.002	0.003	0.002	0.012	0.002	0.002	0.003	0.003	0.003	0.008	0.003
a2p	0.007	0.004	0.005	0.007	0.007	0.028	0.006	0.005	0.008	0.009	0.008	0.014	0.004
c2a	0.009	0.009	0.010	0.010	0.011	-0.021	0.010	0.009	0.011	0.011	0.011	-0.001	0.006
p3pa	0.007	0.005	0.007	0.010	0.009	-0.017	0.008	0.007	0.010	0.010	0.009	0.000	0.007
p3p	0.007	0.006	0.008	0.010	0.010	-0.007	0.008	0.007	0.010	0.011	0.009	0.007	0.007
c2	0.010	0.009	0.012	0.014	0.013	0.016	0.012	0.010	0.015	0.016	0.014	0.025	0.010

Interbond angle (degrees)

basis	C1	C2	C4	C6	C6_P	C6_N	R6	oR6	L13	L13_P	L16	L16_N	oL16
a4p	92.22	91.30	93.56	92.89	101.24	93.43	91.59	96.69	93.50	102.52	93.23	91.57	95.30
p2p	-1.42	-2.01	-1.99	-1.55	-2.95	-2.26	-0.43	-1.60	-3.72	-4.71	-3.85	-2.07	-0.56
a2p	-0.25	-0.14	-0.07	-0.09	-0.24	-0.14	-0.22	-0.41	-0.43	-0.76	-0.43	-0.74	-0.17
c3	-0.08	-0.08	-0.04	-0.06	0.01	-0.06	-0.12	-0.01	-0.10	-0.08	-0.12	-0.22	-0.04
c3a	-0.04	-0.06	-0.05	-0.05	-0.06	0.01	-0.06	-0.02	-0.04	-0.02	-0.05	0.06	-0.05
a3p	-0.19	-0.16	-0.10	-0.01	-0.03	-0.16	-0.14	-0.04	-0.20	-0.19	-0.21	-0.32	-0.04
c4a	0.01	-0.00	-0.00	0.01	-0.01	0.04	-0.00	0.01	0.02	0.03	0.01	0.09	0.02
p3p	-0.51	-0.41	0.06	0.01	0.01	-0.07	-0.19	-0.03	-0.16	-0.52	-0.19	-0.44	-0.02
c4	-0.01	-0.01	0.01	0.01	-0.00	0.03	-0.02	0.04	0.01	-0.01	0.00	-0.00	0.01
p3pa	-0.45	-0.36	0.07	0.02	-0.11	0.02	-0.15	-0.02	-0.07	-0.50	-0.08	-0.14	-0.04
c2a	-0.14	-0.07	-0.05	0.04	-0.30	0.03	-0.12	-0.31	-0.16	-0.45	-0.14	-0.22	-0.23
c2	-0.31	-0.20	0.06	0.10	-0.04	-0.24	-0.29	-0.30	-0.31	-0.74	-0.32	-0.71	-0.13

Binding energy wrt C1 and C2 (eV/pnictogen)

basis	C1	C2	C4	C6	C6_P	C6_N	R6	oR6	L13	L13_P	L16	L16_N	oL16
a4p	0.000	0.000	0.008	0.012	-1.213	0.169	0.007	0.005	0.027	-0.512	0.032	0.118	0.015
c2	0.000	0.000	-0.005	-0.006	0.002	-0.051	-0.006	-0.008	-0.009	-0.005	-0.010	-0.020	-0.009
a2p	0.000	0.000	-0.002	-0.002	0.003	-0.046	-0.002	-0.004	-0.003	0.000	-0.003	-0.014	-0.003
p3p	0.000	0.000	-0.000	-0.001	-0.006	-0.009	-0.002	-0.002	-0.001	-0.005	-0.001	-0.000	-0.001
c3	0.000	0.000	-0.001	-0.001	-0.001	-0.006	-0.001	-0.001	-0.001	-0.001	-0.001	-0.002	-0.001
c4	0.000	0.000	-0.000	-0.000	0.001	-0.000	-0.000	0.000	-0.000	0.000	-0.000	-0.000	0.000
c2a	0.000	0.000	-0.000	0.000	-0.002	0.003	-0.000	-0.001	-0.000	-0.001	-0.000	0.000	0.001
c3a	0.000	0.000	-0.000	0.000	0.000	0.006	-0.000	-0.001	-0.000	-0.001	-0.000	0.001	-0.000
c4a	0.000	0.000	0.000	0.000	0.001	0.005	-0.000	0.000	0.000	0.000	0.000	0.001	0.000
a3p	0.000	0.000	-0.000	0.000	0.003	-0.022	-0.000	-0.000	0.000	0.002	0.001	-0.004	0.001
p3pa	0.000	0.000	0.002	0.002	-0.004	0.008	0.000	-0.000	0.003	-0.001	0.003	0.006	0.004
p2p	0.000	0.000	0.066	0.113	0.093	0.008	0.090	0.095	0.169	0.156	0.187	0.143	0.265

HOMO-LUMO gap (eV)

basis	C1	C2	C4	C6	C6_P	C6_N	R6	oR6	L13	L13_P	L16	L16_N	oL16
a4p	7.758	5.676	4.963	4.627	4.517	2.935	4.819	4.886	4.122	3.955	3.962	1.996	3.686
c2a	-0.636	-0.101	-0.083	-0.045	-0.019	-0.431	-0.065	-0.057	-0.047	-0.013	-0.039	-0.101	-0.023
c3a	-0.639	-0.091	-0.069	-0.042	-0.020	-0.451	-0.053	-0.038	-0.034	-0.021	-0.028	-0.069	-0.023
c4a	-0.645	-0.084	-0.064	-0.039	-0.012	-0.498	-0.048	-0.031	-0.031	-0.016	-0.025	-0.060	-0.020
p3pa	-0.484	-0.058	-0.047	-0.029	0.001	-0.444	-0.031	-0.030	-0.033	0.012	-0.017	-0.075	-0.019
c4	0.106	-0.007	-0.009	-0.005	-0.008	-0.006	-0.004	-0.001	-0.007	-0.011	-0.009	-0.002	-0.004
c3	0.182	0.059	0.049	0.027	-0.006	0.149	0.033	0.026	0.022	-0.002	0.014	0.036	0.014
p3p	0.213	0.104	0.080	0.046	0.007	0.120	0.049	0.038	0.026	0.021	0.025	0.032	0.026
a3p	0.268	0.150	0.127	0.076	0.041	0.238	0.084	0.076	0.063	0.029	0.055	0.099	0.056
c2	0.349	0.216	0.206	0.142	0.033	0.301	0.136	0.097	0.093	0.062	0.087	0.116	0.089
a2p	0.372	0.289	0.307	0.204	0.126	0.430	0.181	0.144	0.158	0.131	0.152	0.170	0.128
p2p	0.465	0.428	0.496	0.416	0.656	0.025	0.193	0.096	0.452	0.566	0.485	-1.295	-0.210

S4 Benchmarking density functionals against CCSD

Table S2: Benchmarking neutral phosphorus clusters. See Section S3 for notations.

d1 - Bond length (Ao)

method	C1	C2	C4	C6	C6_P	C6_N	R6	oR6
CCSD	1.416	2.241	2.240	2.243	2.166	2.759	2.244	2.231
WB97X	-0.002	-0.027	-0.025	-0.023	-0.021	-0.024	-0.025	-0.023
MP2	-0.005	-0.009	-0.011	-0.014	-0.026	-0.143	-0.010	-0.013
PBE0	0.004	-0.013	-0.012	-0.009	0.002	-0.078	-0.013	-0.014
HSE06	0.004	-0.011	-0.010	-0.007	0.005	-0.070	-0.010	-0.012
CAM-B3LYP	-0.002	-0.011	-0.009	-0.005	-0.002	0.039	-0.010	-0.008
APF	0.004	-0.010	-0.008	-0.005	0.007	-0.056	-0.009	-0.010
PBE	0.016	0.010	0.012	0.015	0.032	-0.078	0.011	0.009
B3LYP	0.003	0.013	0.016	0.022	0.030	0.107	0.015	0.015
PBE0-D3	NaN	-0.014	NaN	NaN	NaN	NaN	-0.015	-0.017

a1 - Interbond angle (deg)

method	C1	C2	C4	C6	C6_P	C6_N	R6	oR6
CCSD	93.85	92.85	94.15	93.55	103.46	95.78	93.23	98.70
MP2	-0.11	-0.27	-1.85	-1.78	-0.31	-1.63	-0.49	-0.88
PBE	-1.52	-1.63	-1.00	-1.20	-1.10	-1.64	-1.17	-0.21
PBE0	-0.76	-0.87	-0.53	-0.69	-0.39	-0.72	-0.67	0.23
HSE06	-0.70	-0.90	-0.47	-0.62	-0.49	-0.70	-0.71	0.16
APF	-0.75	-0.85	-0.36	-0.62	-0.44	-0.71	-0.67	0.25
B3LYP	-0.48	-0.55	0.56	0.20	-0.60	-0.12	-0.51	0.53
CAM-B3LYP	-0.19	-0.27	0.65	0.45	0.13	0.43	-0.21	0.81
WB97X	-0.19	-0.28	0.31	0.55	0.87	0.77	-0.17	0.79
PBE0-D3	NaN	-0.86	NaN	NaN	NaN	NaN	-0.67	0.04

Eb - Binding energy wrt [cluster1,chain2] (eV)

method	C1	C2	C4	C6	C6_P	C6_N	R6	oR6
CCSD	0.000	0.000	0.037	0.057	-1.199	0.125	0.050	0.076
B3LYP	0.000	0.000	-0.025	-0.043	-0.011	0.020	-0.040	-0.042
CAM-B3LYP	0.000	0.000	-0.023	-0.039	-0.026	0.007	-0.039	-0.034
APF	0.000	0.000	-0.016	-0.029	-0.003	0.023	-0.027	-0.027
PBE0	0.000	0.000	-0.013	-0.024	0.002	0.023	-0.026	-0.025
HSE06	0.000	0.000	-0.013	-0.024	0.005	0.026	-0.026	-0.026
WB97X	0.000	0.000	-0.013	-0.021	-0.026	0.013	-0.033	-0.024
PBE	0.000	0.000	-0.009	-0.019	0.030	0.038	-0.022	-0.029
MP2	0.000	0.000	0.040	0.064	0.041	0.059	0.059	0.054

f1 - Lowest vibrational frequency (icm)

method	C1	C2
CCSD	1044.1	79.1
WB97X	-25.3	8.2
HSE06	-40.2	12.9
CAM-B3LYP	-17.8	-1.9
B3LYP	-22.6	1.2
PBE	-67.4	11.6
PBE0	-40.7	3.1
MP2	-8.3	6.5
APF	-39.2	4.4

f2 - Second lowest vibrational frequency (icm)

method	C1	C2
CCSD	1167.1	450.0
WB97X	-11.3	22.1
HSE06	-32.8	-0.9
CAM-B3LYP	-12.1	1.6
B3LYP	-25.5	-25.4
PBE	-71.3	-25.3
PBE0	-32.7	2.0
MP2	9.0	7.5
APF	-33.0	-2.0

Table S3: Benchmarking charged phosphorus clusters.

IP - Vertical ionization potential (eV)

method	C1	C2	C6
CCSD	10.392	9.045	7.923
PBE	0.149	-0.072	-0.322
B3LYP	0.185	0.010	-0.242
HSE06	0.091	-0.027	-0.174
APF	0.121	-0.004	-0.163
PBE0	0.096	-0.020	-0.155
CAM-B3LYP	0.148	0.038	-0.093
WB97X	0.114	0.057	0.049
MP2	-0.036	0.098	0.237

EA - Vertical electron affinity (eV)

method	C1	C2	C6
CCSD	-3.243	-1.885	-0.953
WB97X	0.091	-0.504	0.034
CAM-B3LYP	0.363	-0.245	0.261
MP2	-0.026	-0.010	0.364
PBE0	0.457	0.298	0.521
APF	0.480	0.327	0.553
HSE06	0.465	0.316	0.558
B3LYP	0.463	0.381	0.580
PBE	0.600	0.432	0.795

dP - Cation contracted bond length (Ao)

method	C6
CCSD	2.166
MP2	-0.026
WB97X	-0.021
CAM-B3LYP	-0.002
PBE0	0.002
HSE06	0.005
APF	0.007
B3LYP	0.030
PBE	0.032

dN - Anion broken bond length (Ao)

method	C6
CCSD	2.759
MP2	-0.143
PBE0	-0.078
PBE	-0.078
HSE06	-0.070
APF	-0.056
WB97X	-0.024
CAM-B3LYP	0.039
B3LYP	0.107

aP - Cation interbond angle at contracted bond (deg)

method	C6
CCSD	103.46
PBE	-1.10
B3LYP	-0.60
HSE06	-0.49
APF	-0.44
PBE0	-0.39
MP2	-0.31
CAM-B3LYP	0.13
WB97X	0.87

aN - Anion interbond angle at broken bond (deg)

method	C6
CCSD	95.78
PBE	-1.64
MP2	-1.63
PBE0	-0.72
APF	-0.71
HSE06	-0.70
B3LYP	-0.12
CAM-B3LYP	0.43
WB97X	0.77

Table S4: Differential quantities are more sensitive to density functional. Here the first subtable contains energy difference between hydrogen-passivated rings of blue- and black-P (a negative value means that black-P ring has lower energy). The bond 'd1' is out-of-plane bond, 'd2' is in-plane bond, 'a1' is the angle between 'd2' bonds, 'a2' is the angle between 'd1' and 'd2' bonds.

dE - Conformational energy difference per atom (eV)

method	oR6
CCSD	-0.0134
WB97X	-0.0044
CAM-B3LYP	-0.0026
PBE0-D3	-0.0017
PBE0	-0.0005
HSE06	-0.0003
APF	-0.0001
B3LYP	0.0012
MP2	0.0022
PBE	0.0033

d21 - Bond length difference d1-d2 (Ao)

method	oR6
CCSD	0.0119
MP2	-0.0020
PBE0-D3	-0.0003
HSE06	0.0008
PBE0	0.0009
PBE	0.0010
APF	0.0014
WB97X	0.0028
CAM-B3LYP	0.0036
B3LYP	0.0049

a12 - Interbond angle difference a2-a1 (deg)

method	oR6
CCSD	1.56
PBE0-D3	-0.49
PBE0	-0.30
WB97X	-0.20
MP2	-0.18
APF	-0.18
HSE06	-0.10
CAM-B3LYP	-0.05
PBE	0.17
B3LYP	0.45

PRE - Hole polaron relaxation energy (eV)

method	C6
CCSD	0.389
B3LYP	-0.047
PBE	-0.029
CAM-B3LYP	-0.014
APF	-0.007
HSE06	-0.004
PBE0	0.001
WB97X	0.017
MP2	0.101

NRE - Electron polaron relaxation energy (eV)

method	C6
CCSD	1.360
PBE	-0.450
MP2	-0.392
HSE06	-0.260
APF	-0.242
PBE0	-0.237
B3LYP	-0.203
CAM-B3LYP	0.014
WB97X	0.167

S5 Benchmarking density functionals by Koopman's theorem

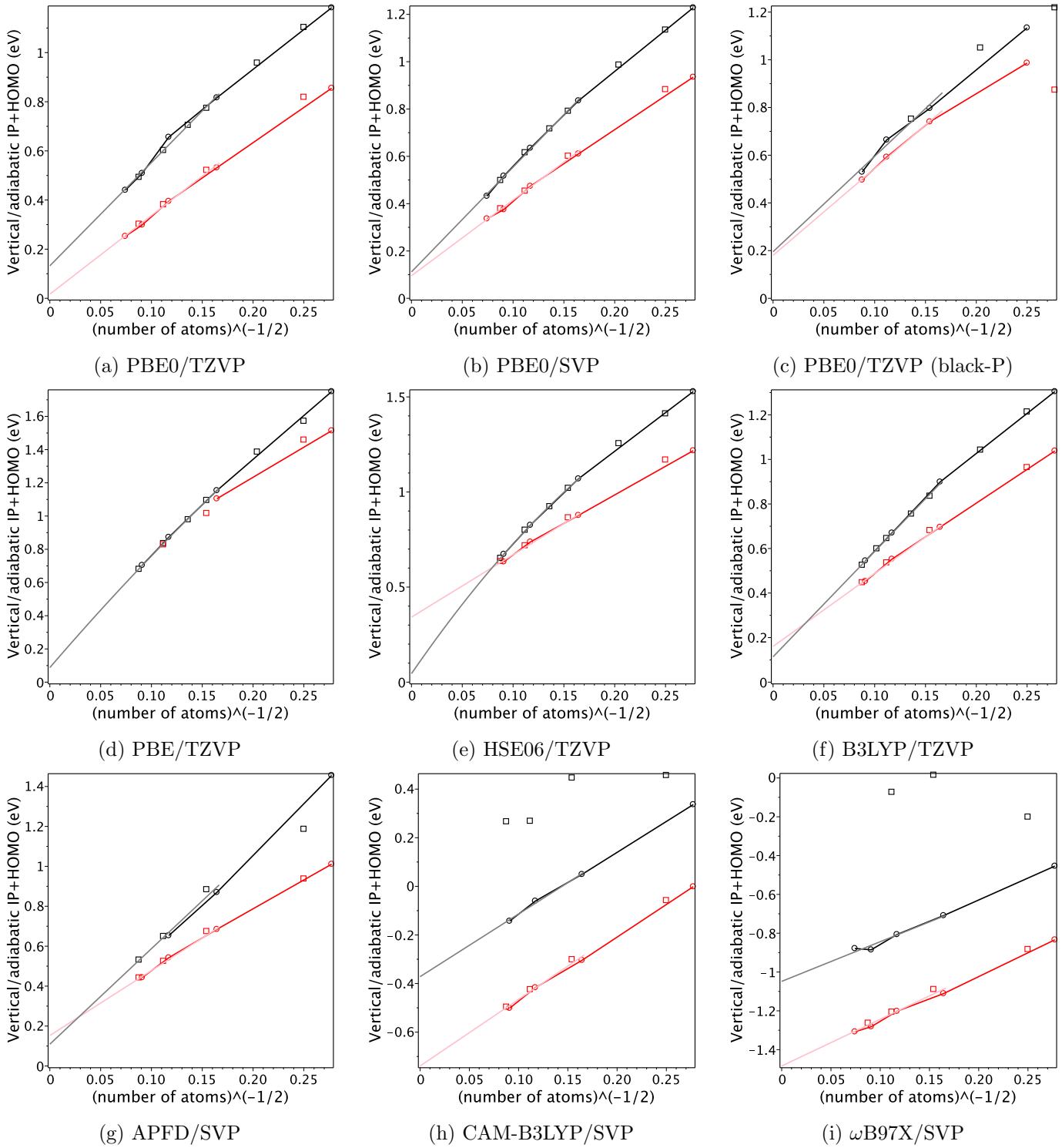

(a) PBE0/TZVP (b) PBE0/SVP (c) PBE0/TZVP (black-P)

(d) PBE/TZVP (e) HSE06/TZVP (f) B3LYP/TZVP

(g) APFD/SVP (h) CAM-B3LYP/SVP (i) ωB97X/SVP

Figure S11: Sum of the vertical (black dots) or adiabatic (red dots) IP and HOMO energies for all considered density functionals for blue phosphorene clusters except for panel (c).

S6 Main parameters of blue- and black-P monolayers

Table S5: Main parameters of blue- and black-P monolayers. Data are grouped by basis set: a3p=def2-TZVP, a2p=def2-SVP, paw400=PAW method with 400 eV cutoff. Density functionals are ordered by the band gap. Black-P data are marked by asterisk '*', blue-P data have no asterisk. NBO energies are calculated for 96-atom clusters: energies of LP orbitals are absolute, those of bonding orbitals are relative to the LP. In case of CAM-B3LYP and ωB97 functionals with def2-TZVP basis, the wave-function is not converging for black-P at the default for Gaussian 16 precision.

Method	dE	bondlengths		angles		gap	HOMO	LUMO	LP	bonding orbitals		
	meV	Ao	Ao	deg	deg	eV	eV	eV	eV	eV	eV	
--- paw400 ---												
PBE		2.261		92.9		1.93	-4.29	-2.36				
	-1.6	2.258	2.221	96.0	104.1	0.91	-2.84	-1.93				*
PBE0		2.234		93.3		3.39	-5.19	-1.80				
	-7.1	2.229	2.197	96.5	104.1	2.21	-3.50	-1.29				*
--- a3p ---												
PBE		2.265		92.8		1.94	-6.17	-4.23	-13.48	1.22		
	-4.5	2.263	2.224	95.9	104.1	0.92	-5.05	-4.12	-12.20	-0.32	-0.81	*
HSE06		2.243		93.3		2.70	-6.75	-4.04	-14.19	0.54		
	-11.3	2.239	2.204	96.5	104.3	1.63	-5.48	-3.86	-12.77	-1.23	-1.72	*
B3LYP		2.271		94.1		3.10	-6.79	-3.69	-14.33	1.00		
	-2.4	2.272	2.226	96.8	105.4	2.16	-5.65	-3.49	-12.98	-0.58	-1.18	*
APF		2.244		93.3		3.28	-7.05	-3.77	-14.46	0.54		
	-8.7	2.238	2.205	96.4	104.3	2.19	-5.77	-3.58	-13.02	-1.27	-1.74	*
PBE0		2.241		93.2		3.40	-7.12	-3.72	-14.53	0.45		
	-9.6	2.234	2.202	96.4	104.2	2.28	-5.81	-3.53	-13.08	-1.40	-1.85	*
CAM-B3LYP		2.245		94.3		5.44	-8.15	-2.72	-15.57	0.14		
									-14.07	-1.74	-2.25	*
WB97X		2.230		94.2		7.21	-9.23	-2.02	-16.41	-0.45		
									-14.80	-2.47	-2.95	*
--- a2p ---												
PBE		2.291		92.4		2.10	-6.29	-4.19	-13.91	2.08		
	2.4	2.289	2.251	95.8	102.7	0.83	-5.18	-4.34	-12.77	0.59	0.14	*
HSE06		2.268		92.8		2.89	-6.90	-4.01	-14.73	1.43		
	-3.9	2.263	2.228	96.3	103.1	1.54	-5.65	-4.11	-13.44	-0.34	-0.82	*
B3LYP		2.294		93.6		3.26	-6.83	-3.57	-14.75	1.86		
	10.6	2.294	2.250	96.5	104.2	2.13	-5.75	-3.63	-13.54	0.32	-0.23	*
APF		2.269		92.8		3.46	-7.22	-3.76	-15.02	1.43		
	-0.5	2.264	2.229	96.3	103.1	2.09	-5.95	-3.86	-13.71	-0.37	-0.83	*
PBE0		2.266		92.7		3.58	-7.30	-3.71	-15.10	1.35		
	-2.6	2.260	2.226	96.3	103.0	2.18	-5.99	-3.81	-13.77	-0.50	-0.95	*
CAM-B3LYP		2.267		93.8		5.62	-8.20	-2.58	-16.08	1.00		
	2.0	2.263	2.227	96.9	104.1	4.32	-6.88	-2.56	-14.70	-0.84	-1.33	*
WB97X		2.251		93.8		7.41	-9.32	-1.91	-16.95	0.31		
	-11.8	2.246	2.210	97.3	104.2	5.94	-7.84	-1.89	-15.45	-1.70	-2.19	*

Table S6: Tight-binding parameters of the valence band of blue- and black-P monolayers (in meV) derived from the Fock matrix of 96-atom clusters using NBO orbitals to project MOs onto LMOs. Here sites are numbered by the chemical distance, LP=lone pair, BD=bonding orbital (see Fig.3d), prime denotes in-plane bonds in black-P, r/o denotes blue/black allotrope. Site labels 'p' and 'o' have the following meaning: 'p' denotes sites which are closer to a chain of bonds along vectors $\boldsymbol{a'}$, $\boldsymbol{b}$, $\boldsymbol{b'}$ in Fig.1 (path of the strongest connectivity), whereas 'o' means opposite sites in 6-membered rings. Only sites closer than 4th neighbor and with couplings stronger than 50 meV are listed comprehensively.

site	LP	r	o	site	BD	r	o	site	BD'	o
0		-11770	-11090	0		-12793	-12895	0		-13360
1	BD	-2505	-2497	1	LP	-2505	-2497			
1	BD'		-2453					1	LP	-2453
				1	BD	-1438		1	BD'	-1645
				1	BD'		-1325	1	BD	-1325
1	LP	515	504							
			-115							
2	BD	-335	591	2	LP	-335	591			
2	BD'		-277					2	LP	-277
			-270							-270
				2	BD	565	-405	2	BD'	521
										467
										-177
				2	BD'	-266	-213	2	BD	-213
2	LP	-116	135							
			-115							
3p	LP	-147	-473							
			174							
			-59							
3o	LP	41	98							
				3p	BD	62	<20	3p	BD'	-133
				3o	BD	-175	-114	3o	BD'	-138
				3p	BD'	-142	131	3p	BD	131
				3o	BD'	61	52	3o	BD	52
3p	BD	147	-120	3p	LP	147	-120			
3o	BD	39	70	3o	LP	39	70			
3p	BD'		-183					3p	LP	-183
			100							100
3o	BD'		64					3o	LP	64
----------			selective	----------						
4p	BD'		133					4p	LP	133
4p	BD	-24	-64	4p	LP	-24	-64			
4o	BD	-51	-48	4o	LP	-51	-48			
								4p	BD'	92
				4p	BD	99				
4p	LP	-39	-58							

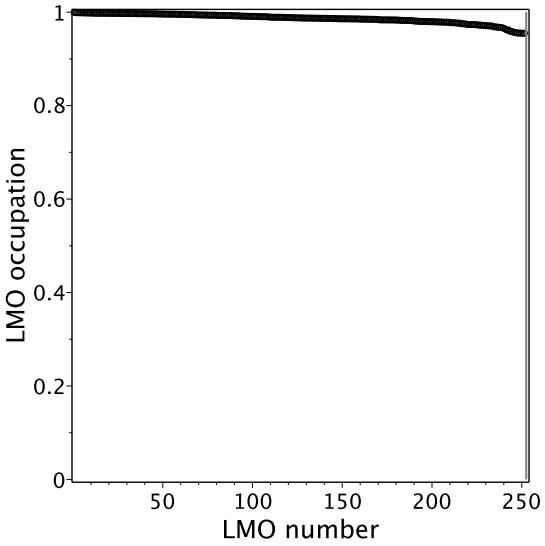

(a) Blue-P hole LMO "occupations".

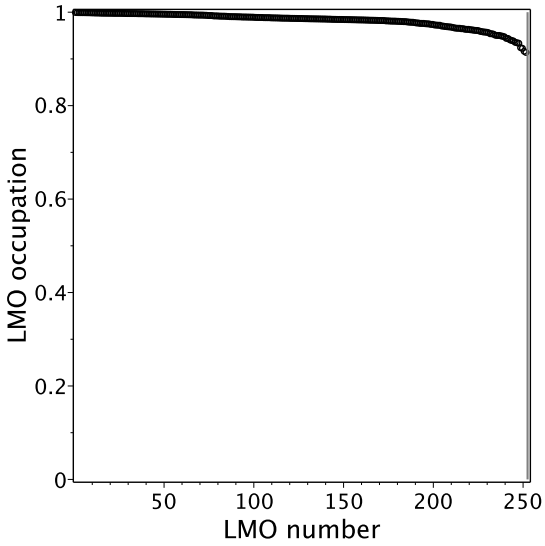

(b) Black-P hole LMO "occupations".

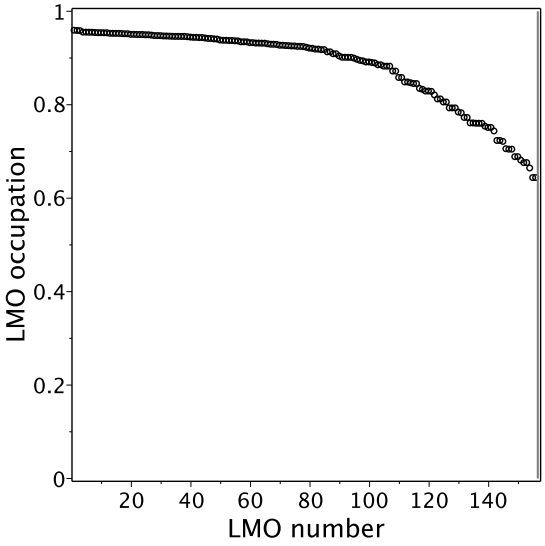

(c) Blue-P electron LMO "occupations".

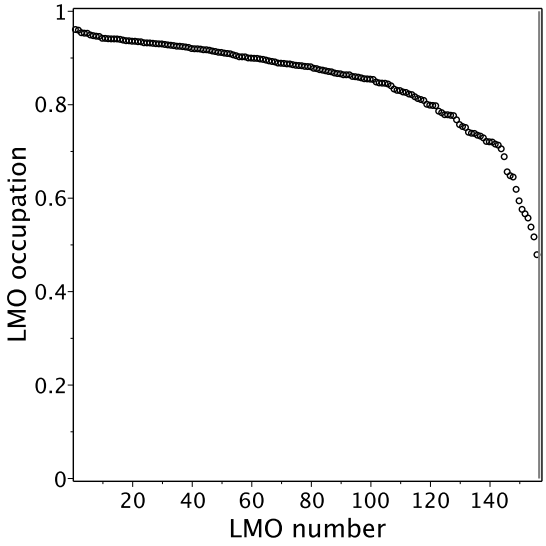

(d) Black-P electron LMO "occupations".

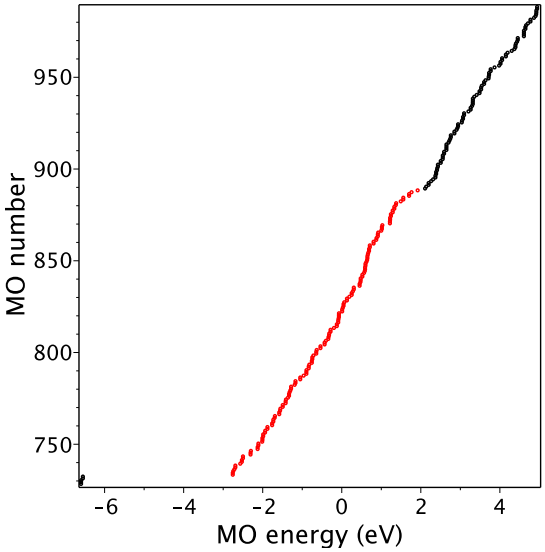

(e) Blue-P MOs used to generate electron LMOs (shown in red).

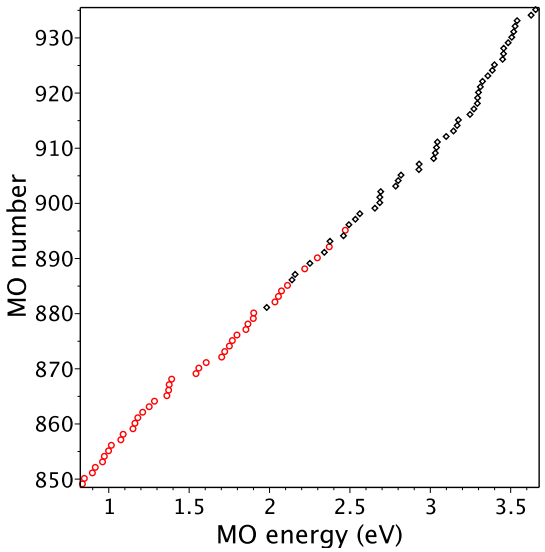

(f) Black-P MOs used to generate electron LMOs (for clarity only boundary region is shown).

Figure S12: Technical details of LMOs. Here "occupations" are singular eigenvalues of the scalar product of selected MOs and NBOs. The shown figures are for 96-atom clusters.

S7 Electronic structure of monolayers

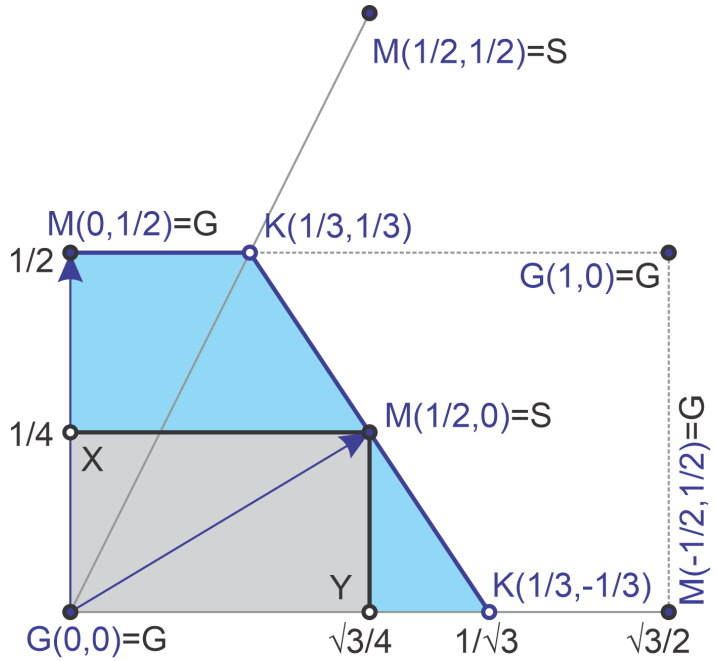

Figure S13: Mapping between k-vectors of rhombohedral (blue-colored) and orthorhombic (black-colored) lattices. Cartesian coordinates are given in fractions of the translation k-vector of the rhombohedral lattice. Lattice coordinates of k-vectors of the rhombohedral lattice are written in blue color. The first quarters of Brillouin zones are shaded with the corresponding color.

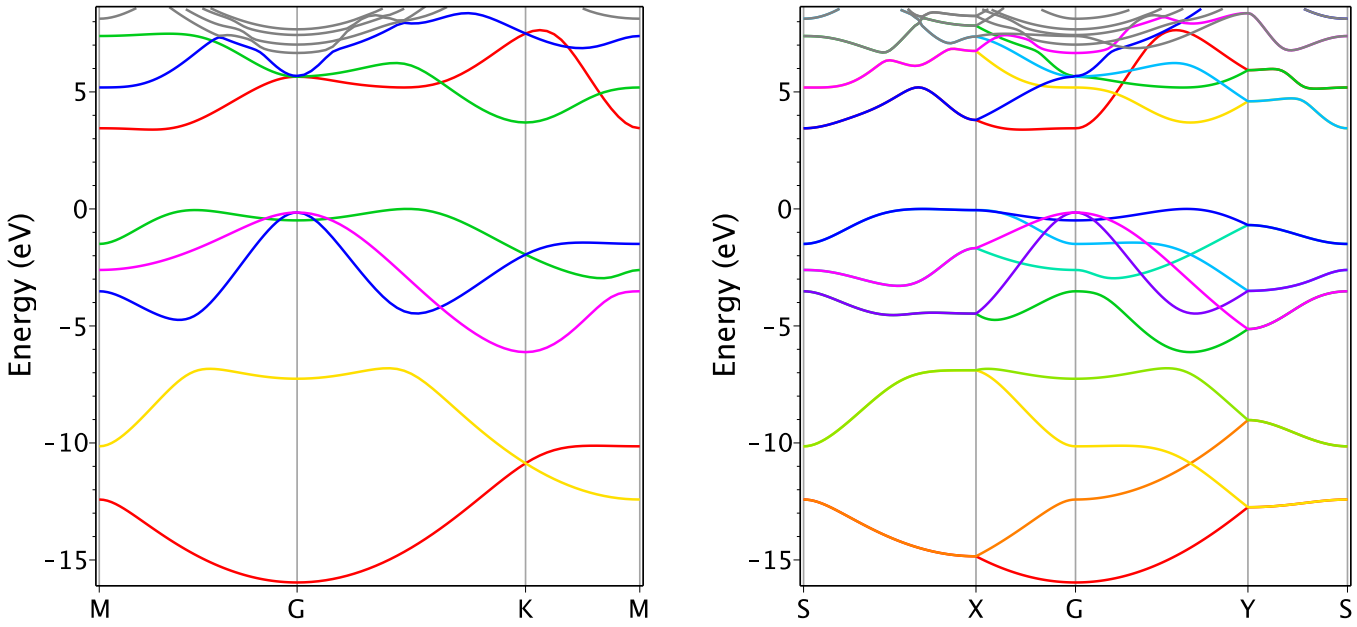

(a) Rhombohedral unit cell.

(b) Orthorhombic unit cell.

Figure S14: Comparison of band structure of blue-P in rhombohedral and orthorhombic unit cells (PBE0/PAW400).

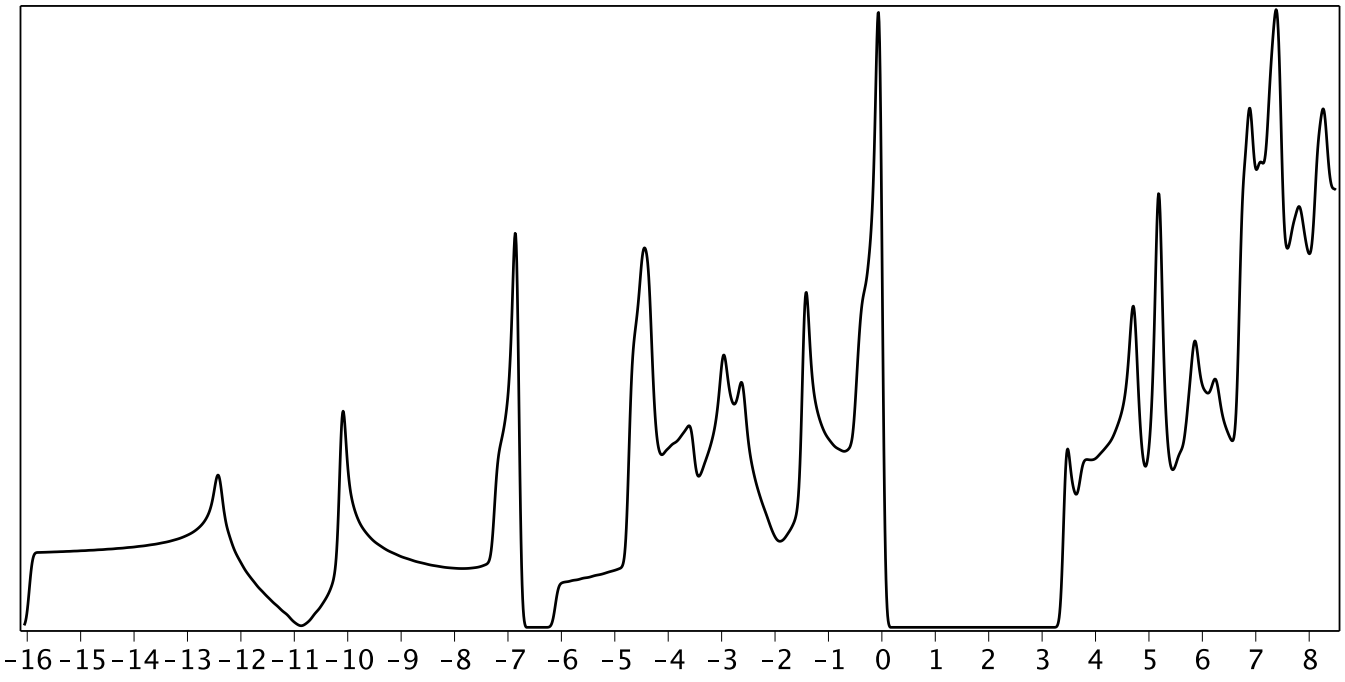

(a) Blue-P.

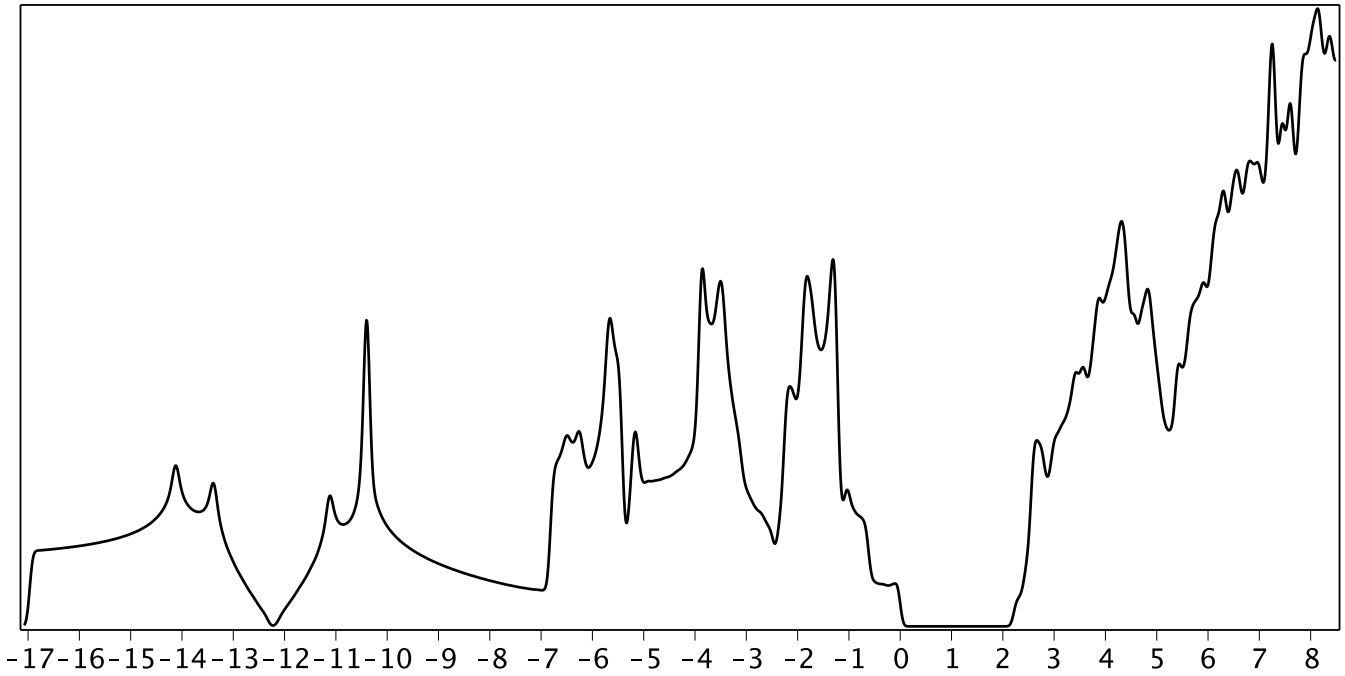

(b) Black-P.

Figure S15: Density of states: blue-P vs black-P (PBE0).

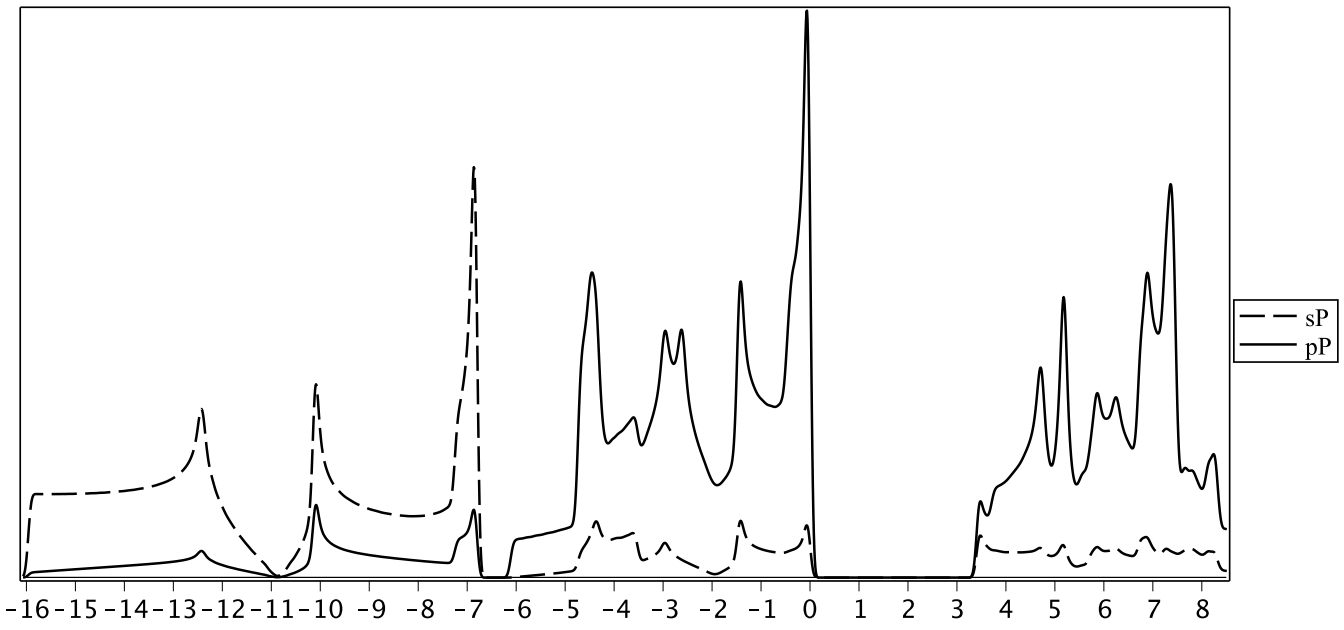

(a) Blue-P.

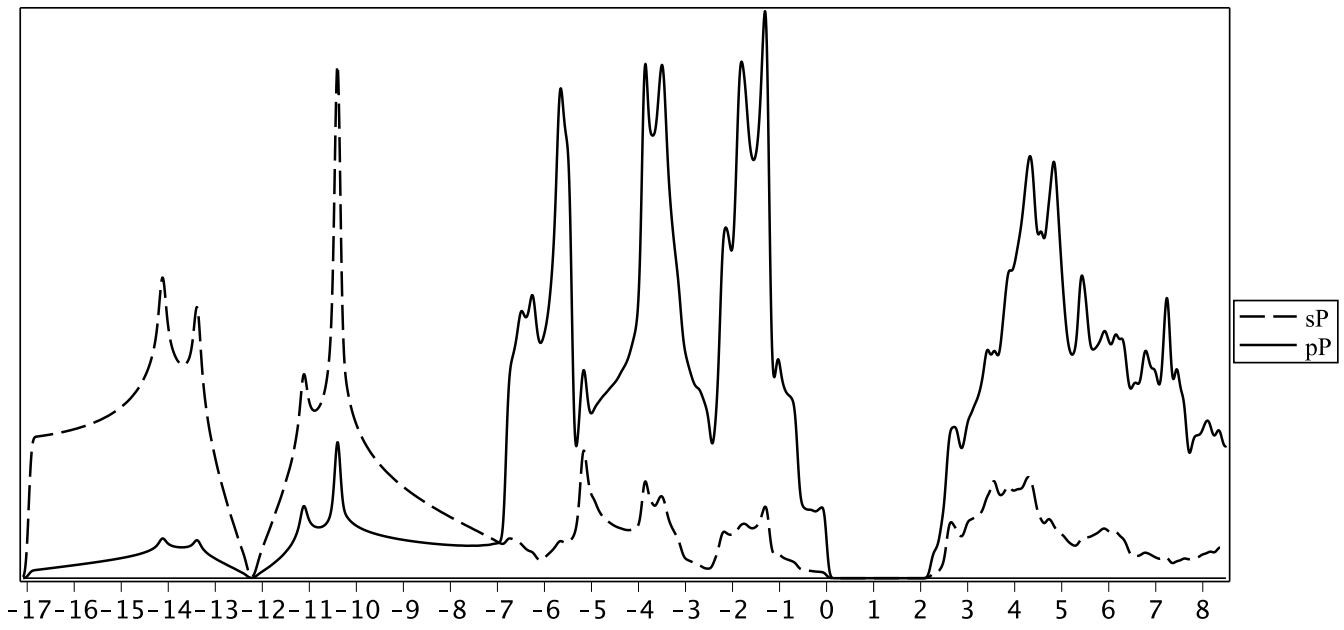

(b) Black-P.

Figure S16: Partial density of states: blue-P vs black-P (PBE0).

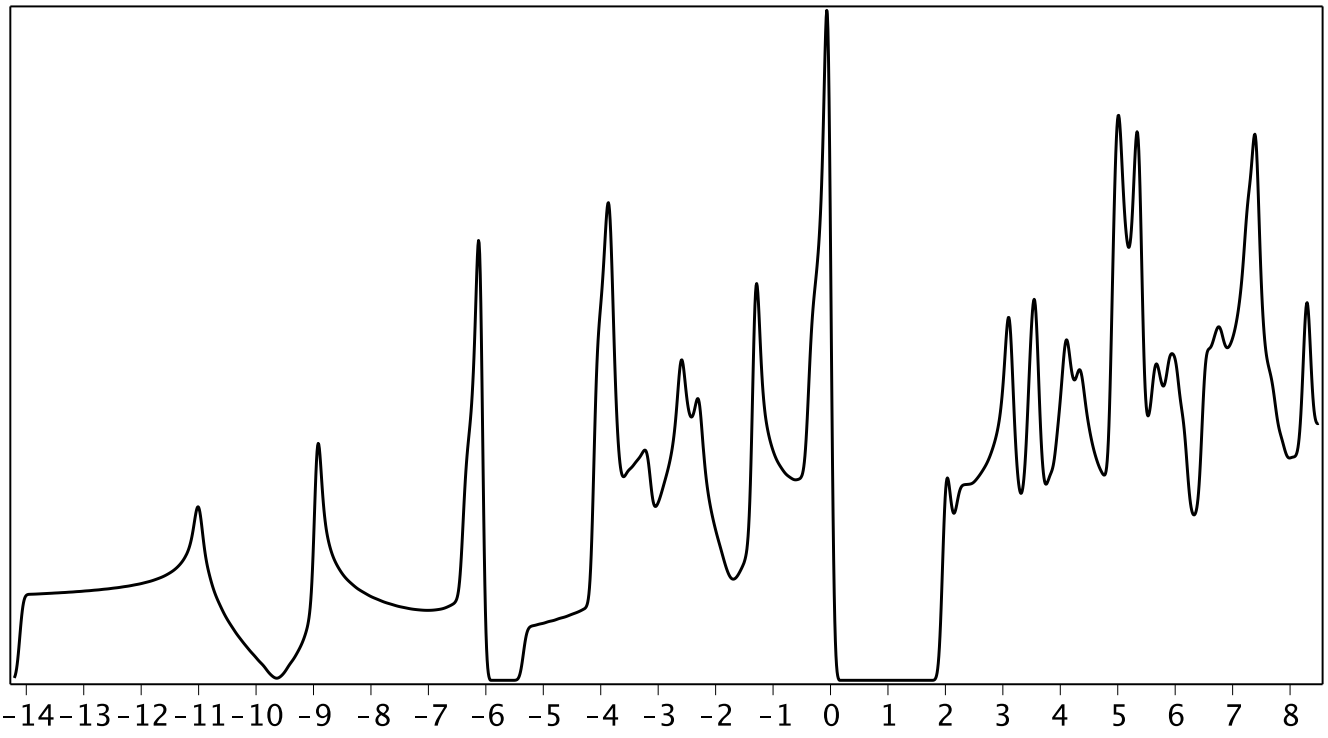

(a) Blue-P.

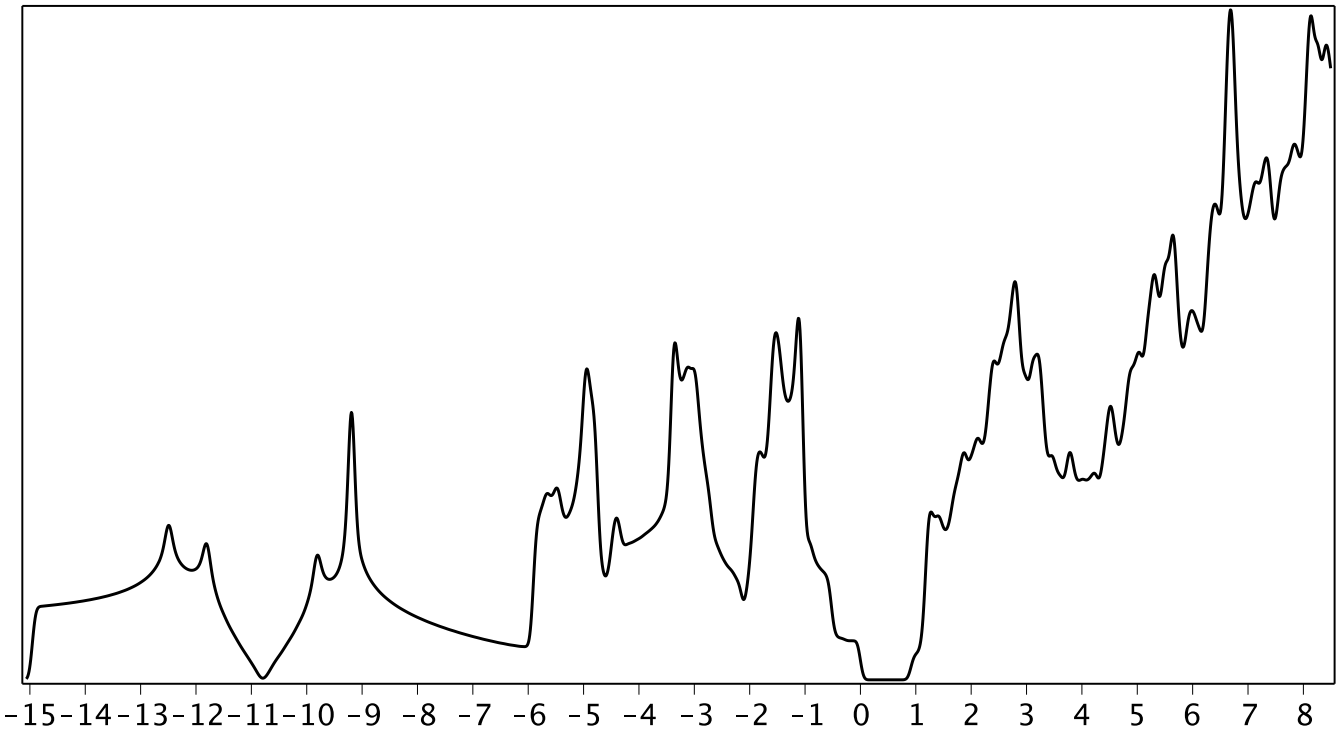

(b) Black-P.

Figure S17: Density of states: blue-P vs black-P (PBE).

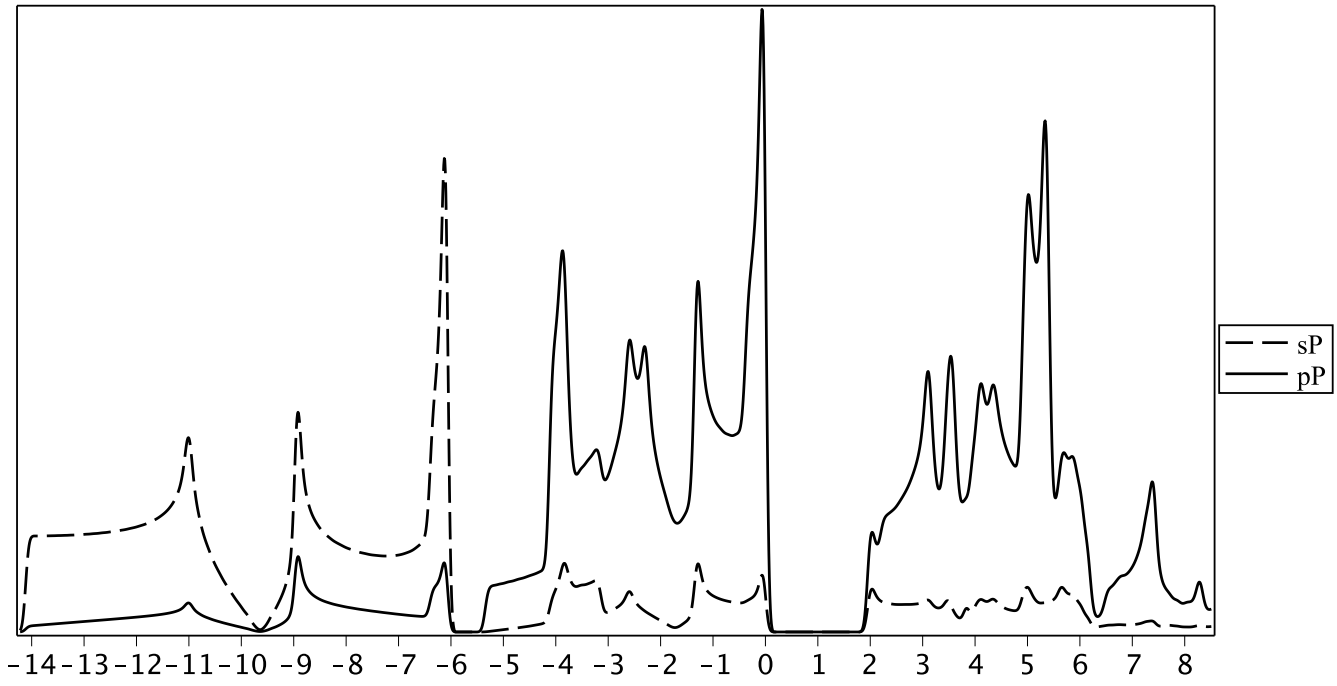

(a) Blue-P.

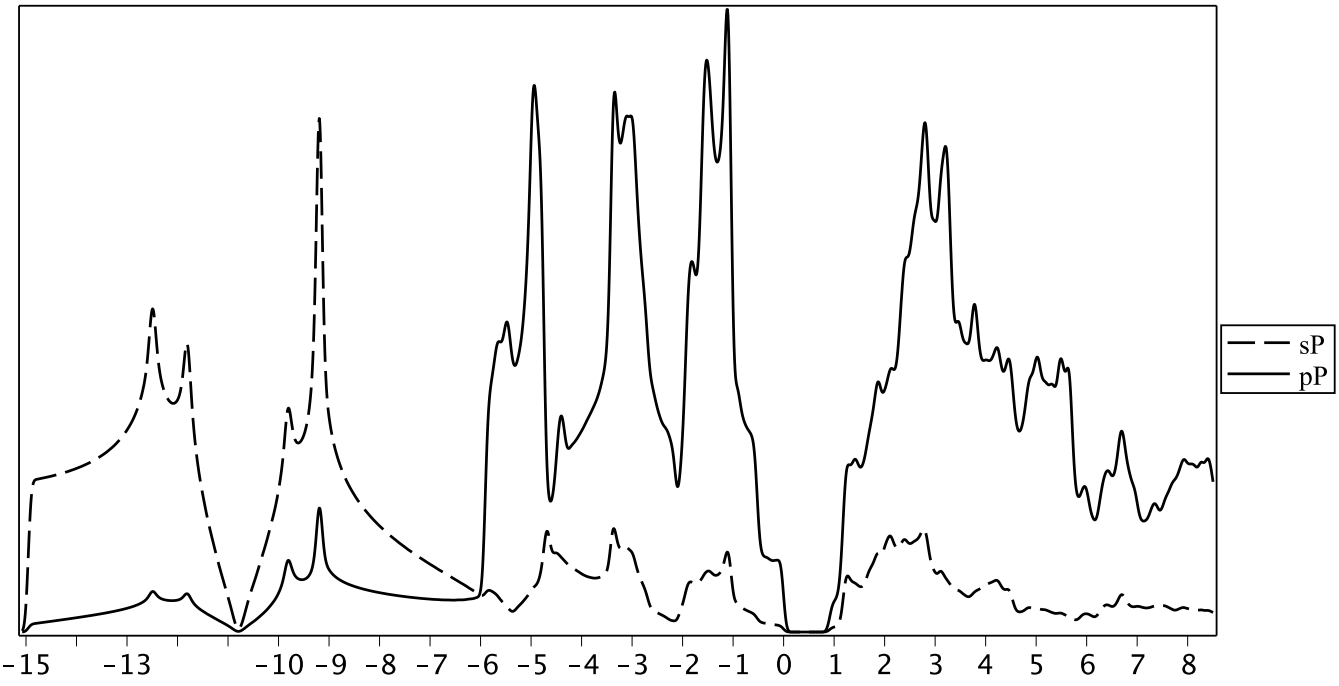

(b) Black-P.

Figure S18: Partial density of states: blue-P vs black-P (PBE).

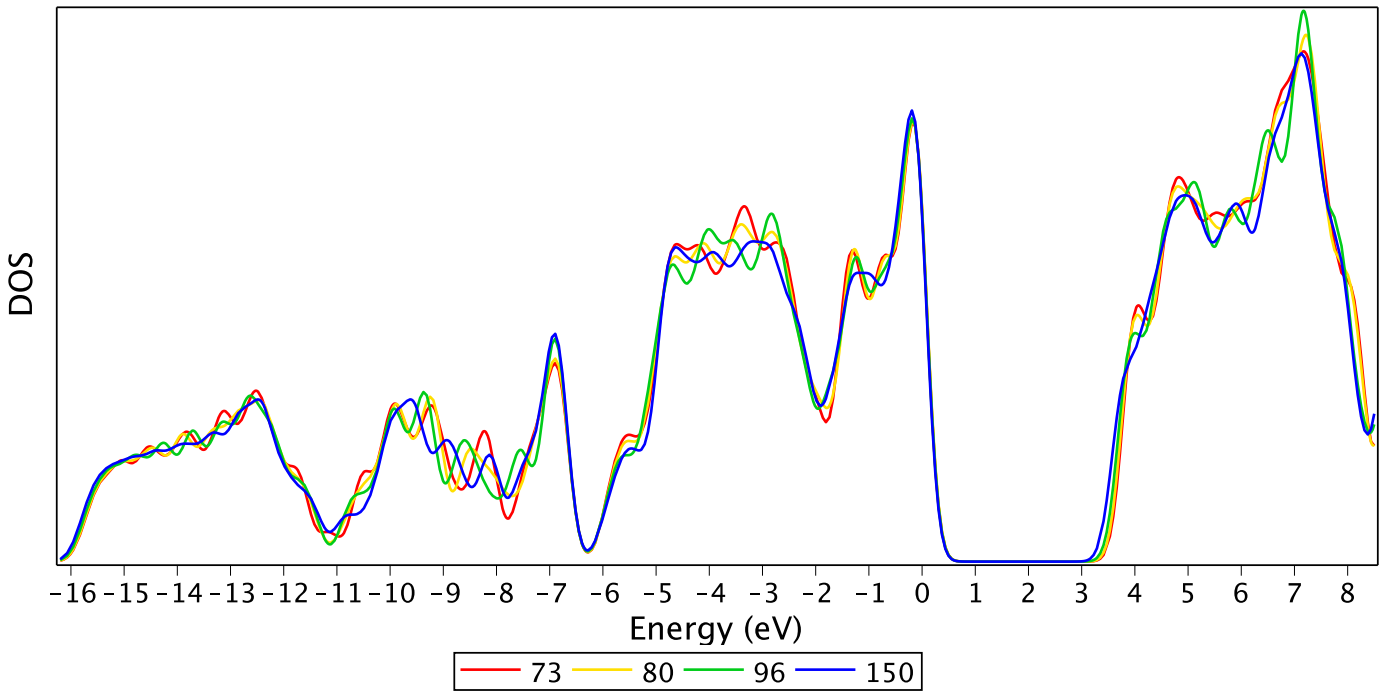

(a) Clusters in TZVP basis.

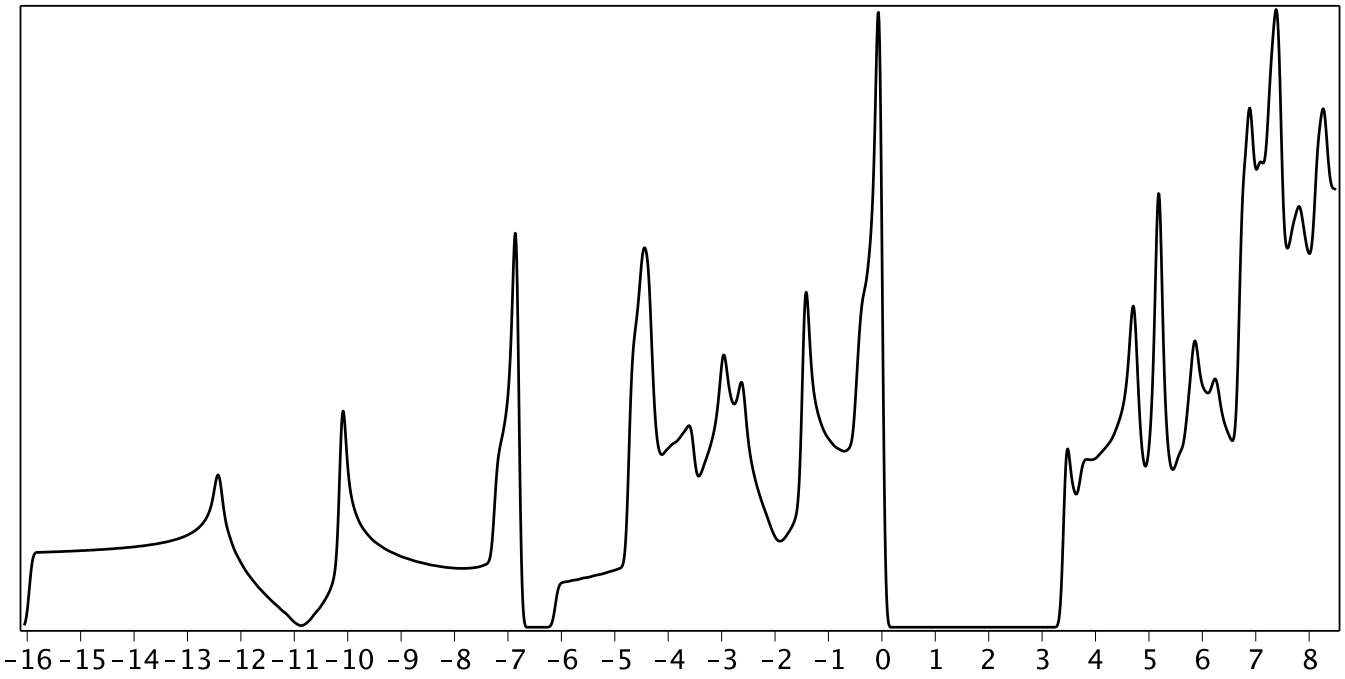

(b) Monolayer in PAW400 basis.

Figure S19: Comparison of DOS of blue-P calculated with PBE0 using cluster approach and plane waves.

S8 Polaron wave-function and lattice deformation

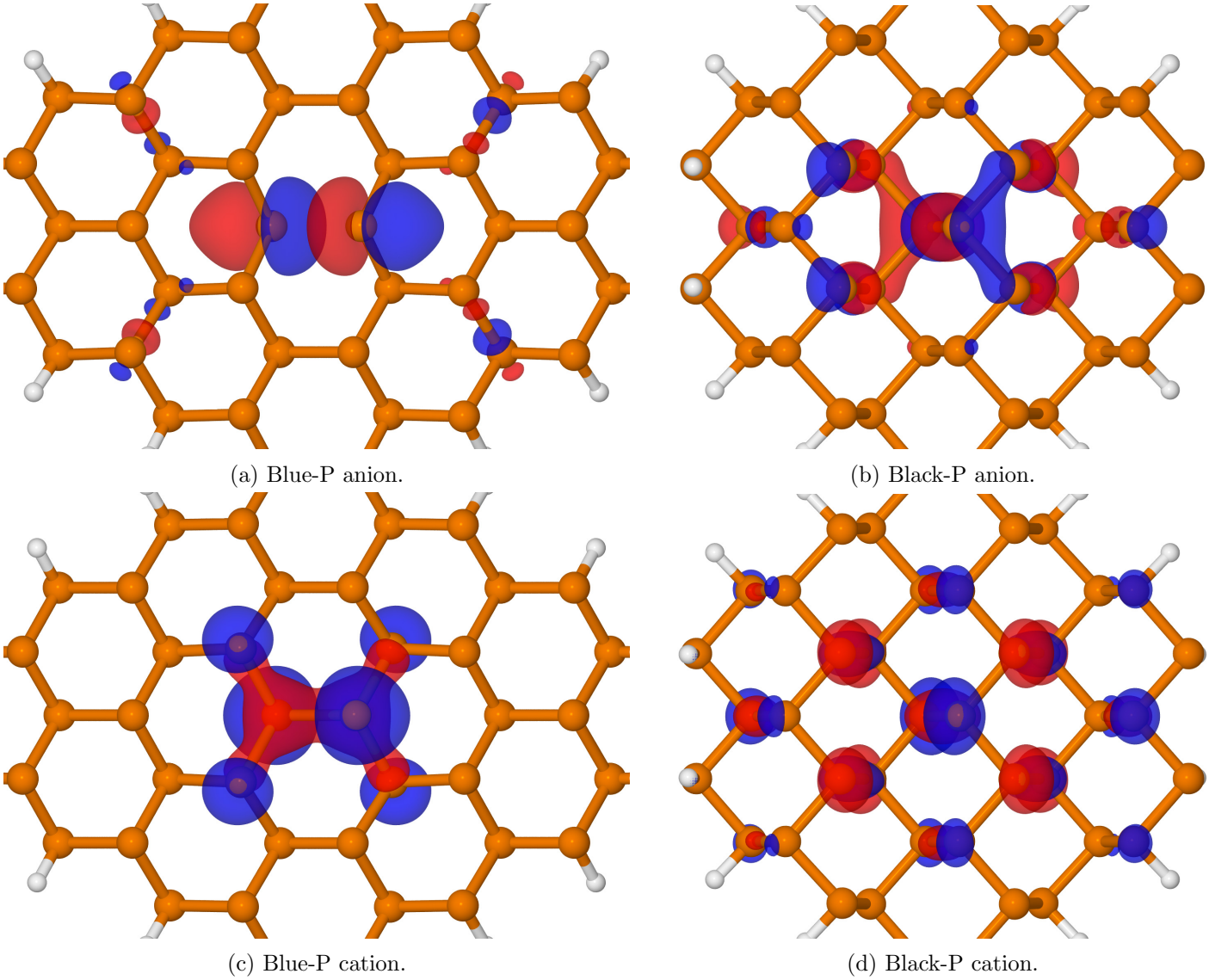

(a) Blue-P anion.

(b) Black-P anion.

(c) Blue-P cation.

(d) Black-P cation.

Figure S20: Natural orbitals of relaxed anions (a,b) and cations (c,d) of hydrogen-passivated 42-atom cluster for blue-P (a,c) and black-P (b,d). In all figures of the current work, the wave-function isovalue is typically 0.05 for LMO and 0.03 for MO. In case of comparison, all figures are plotted with the same isovalue.

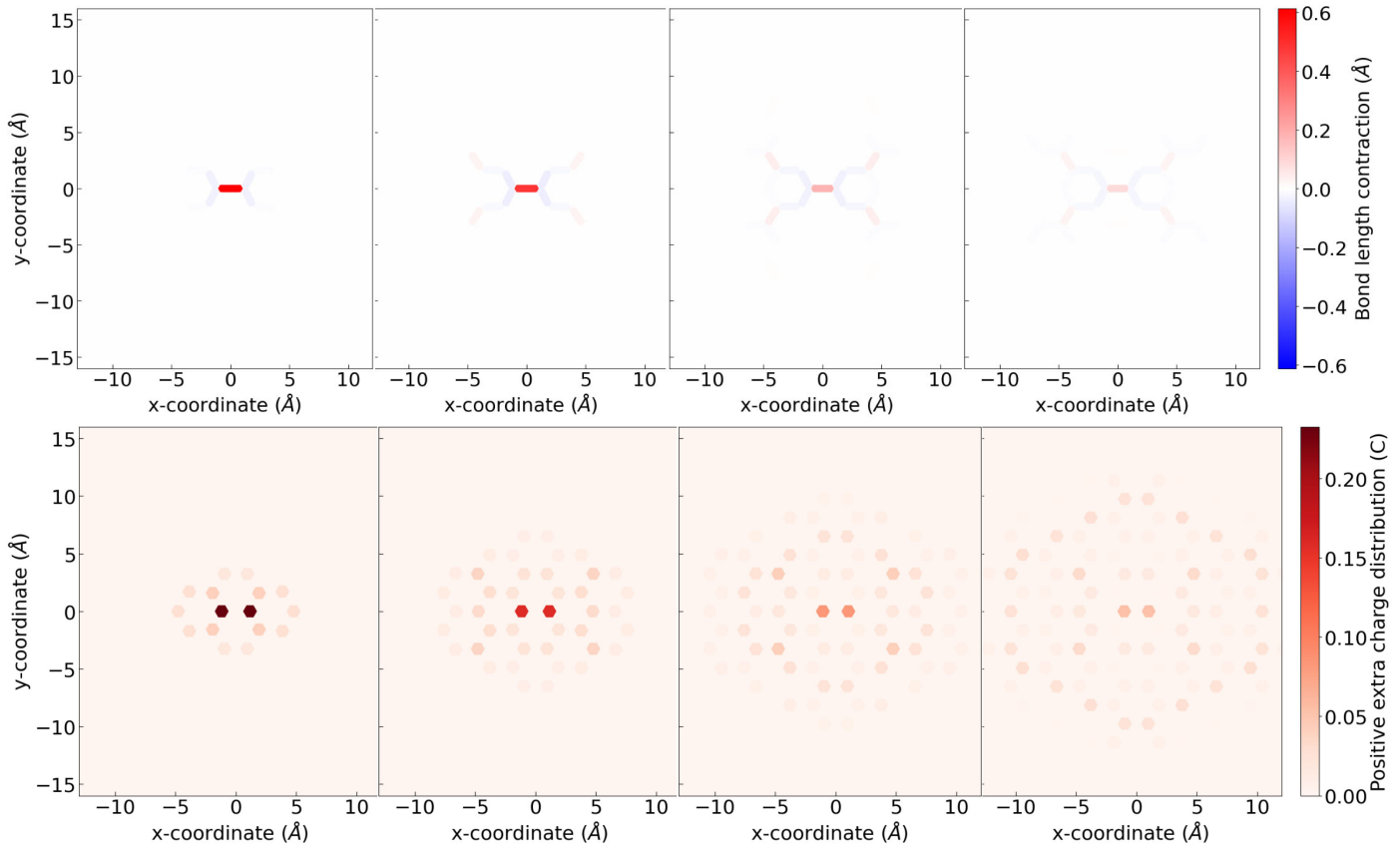

Figure S21: Blue-P bond elongation and negative extra charge distribution profiles for an electron polaron as the number of P atoms in a cluster increases.

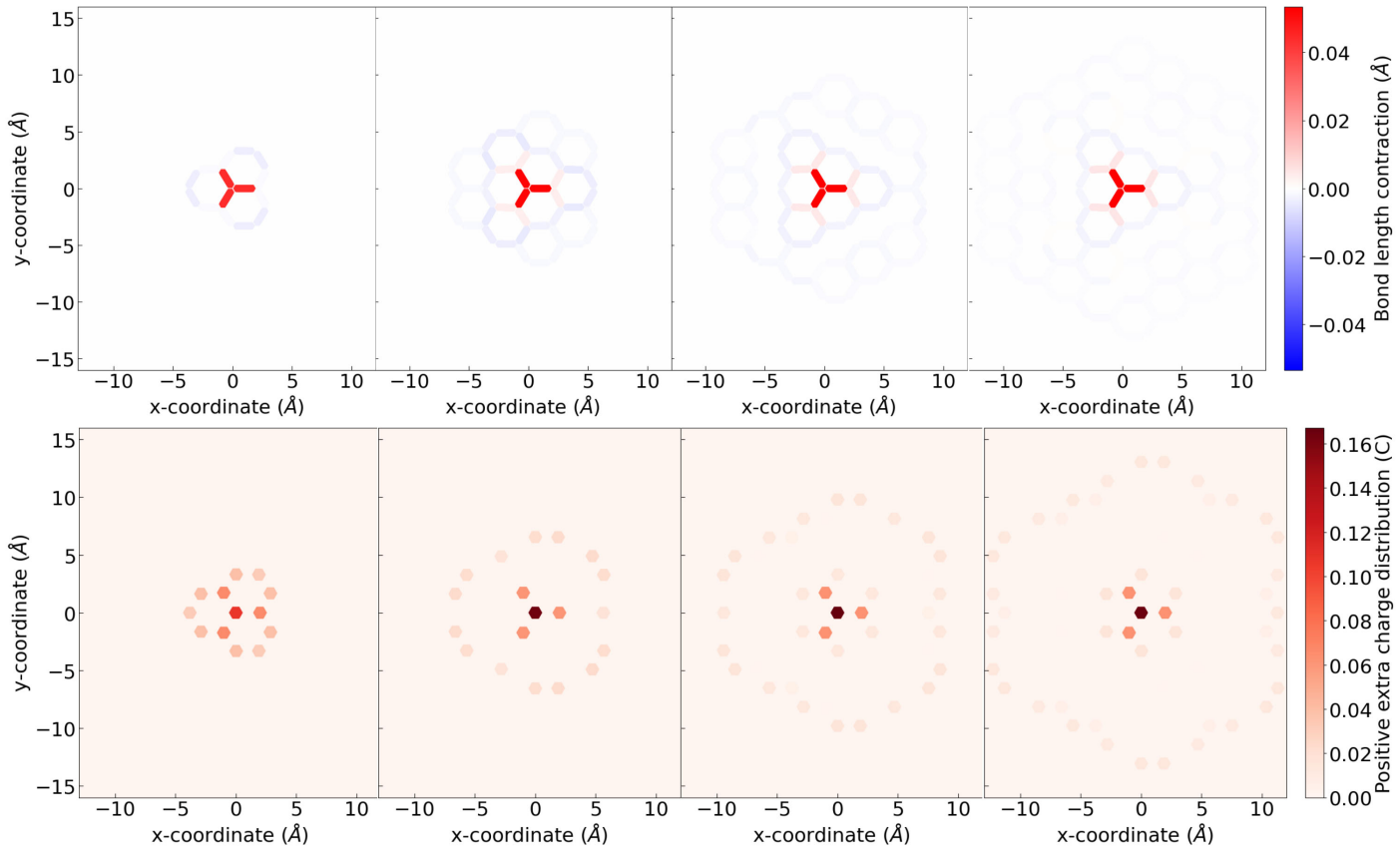

Figure S22: Blue-P bond contraction and positive extra charge distribution profiles for a hole polaron as the number of P atoms in a cluster increases.

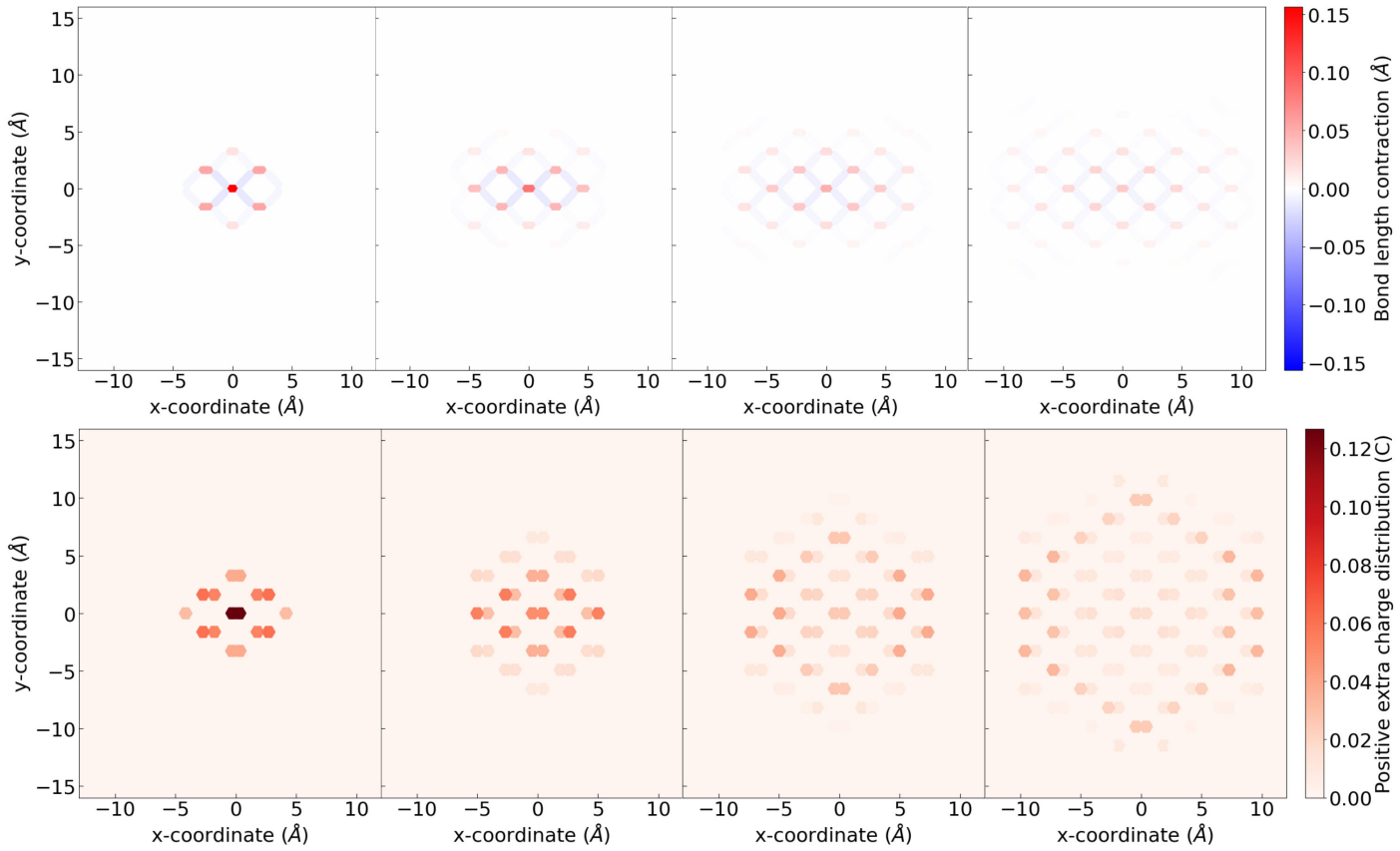

Figure S23: Black-P bond elongation and negative extra charge distribution profiles for an electron polaron as the number of P atoms in a cluster increases.

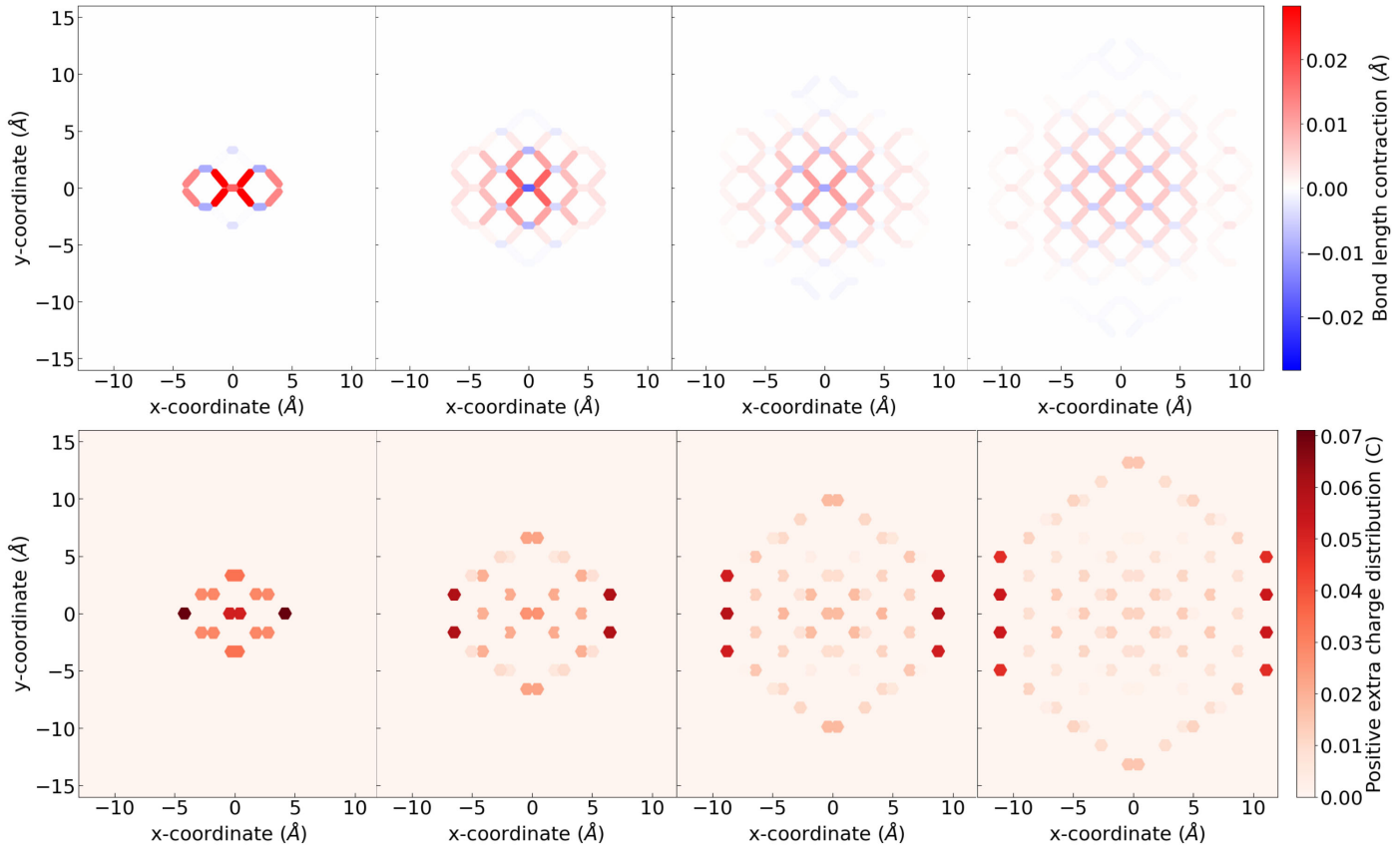

Figure S24: Black-P bond contraction and positive extra charge distribution profiles for a hole polaron as the number of P atoms in a cluster increases.

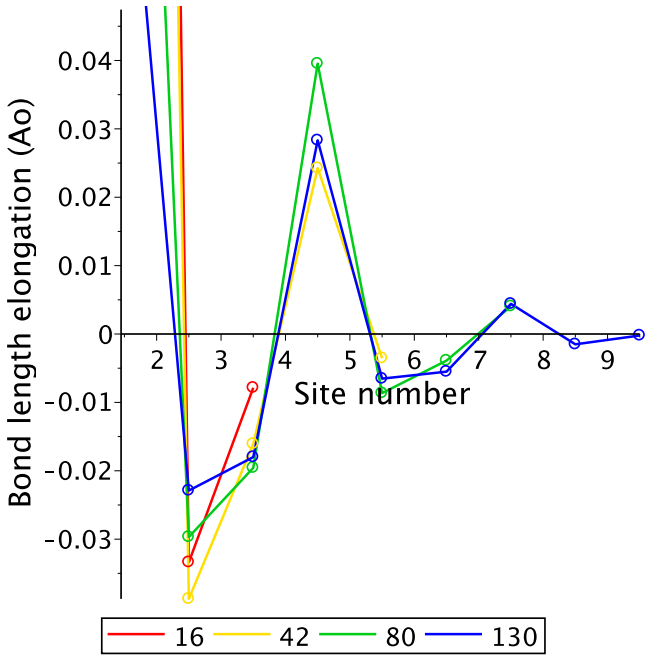

(a) Blue-P anion.

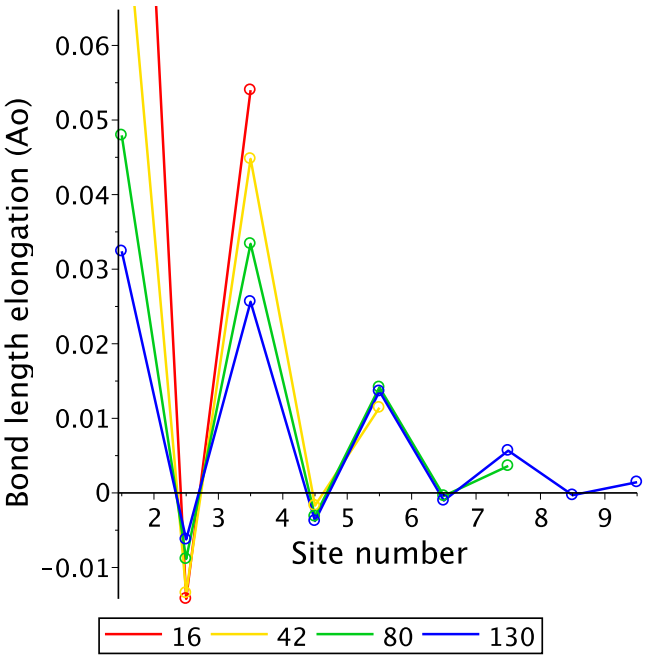

(b) Black-P anion.

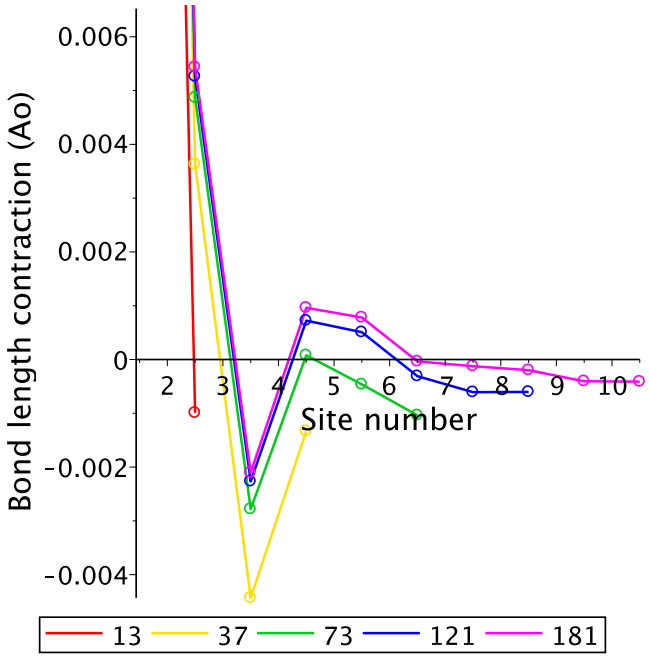

(c) Blue-P cation.

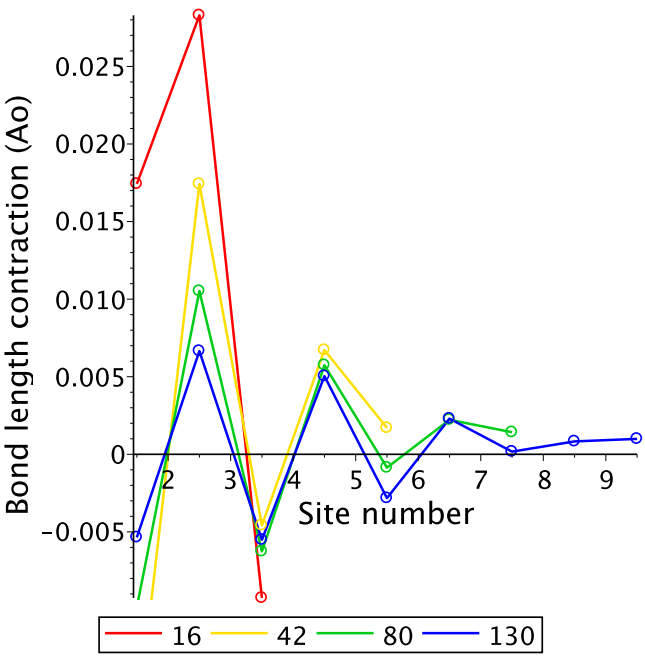

(d) Black-P cation.

Figure S25: Bond length change profiles along a linear path for anions and cations of hydrogen-passivated clusters of various sizes (the size is given in the legends). The change is given with respect to the neutral cluster. The path goes from the center to the edge along $\boldsymbol{a}'$ or symmetry-equivalent translation vectors, e.g., atoms $\{3, 2, 1, 7, 24\}$ in Fig. S1c.

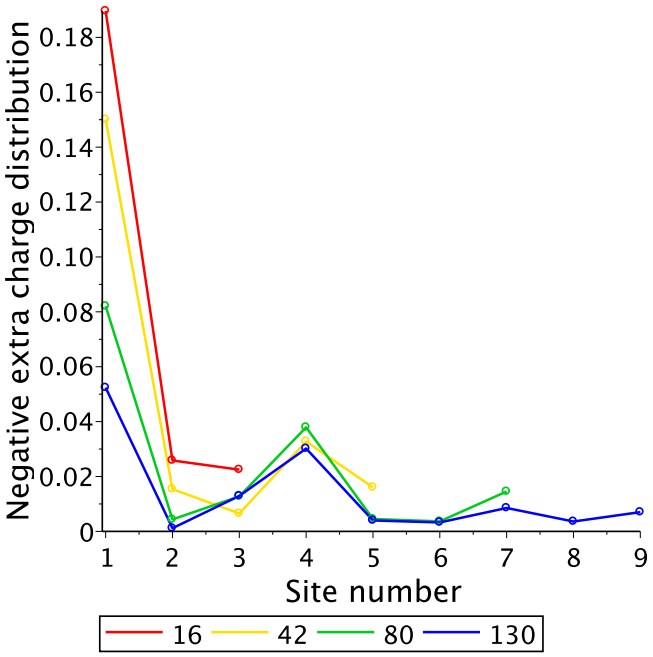

(a) Blue-P anion.

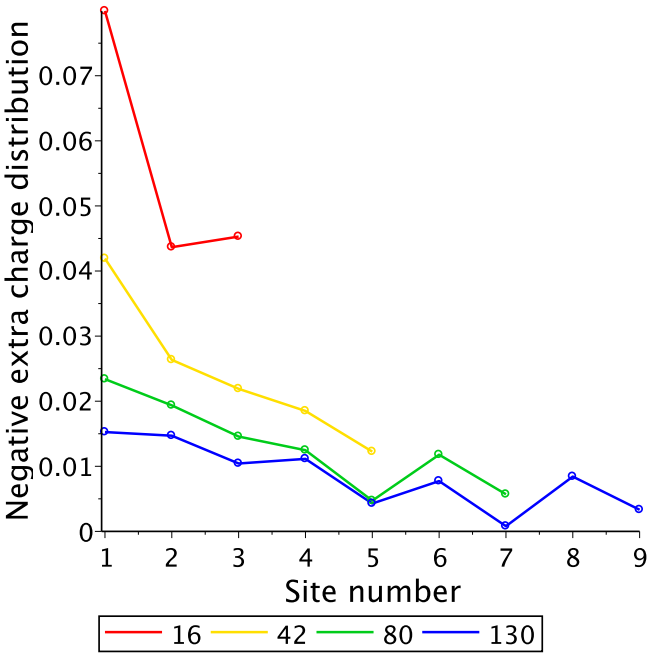

(b) Black-P anion.

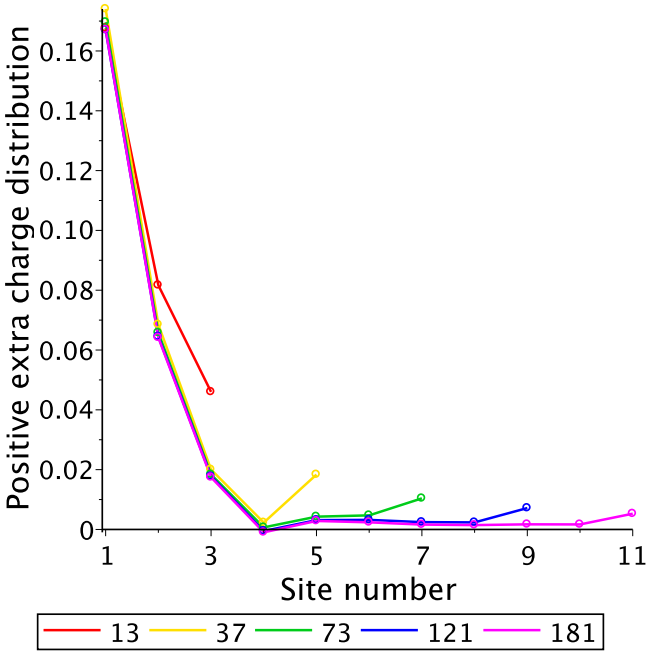

(c) Blue-P cation.

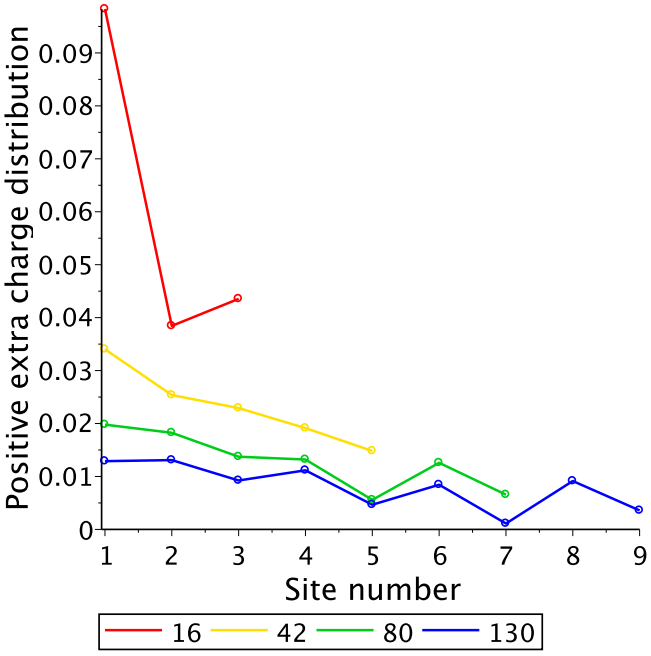

(d) Black-P cation.

Figure S26: Extra charge distribution profiles along a linear path for anions and cations of hydrogen-passivated clusters of various sizes, see details in the previous figure. NBO atomic charges are used here.

S9 Size convergence studies of hole polaron in blue-P

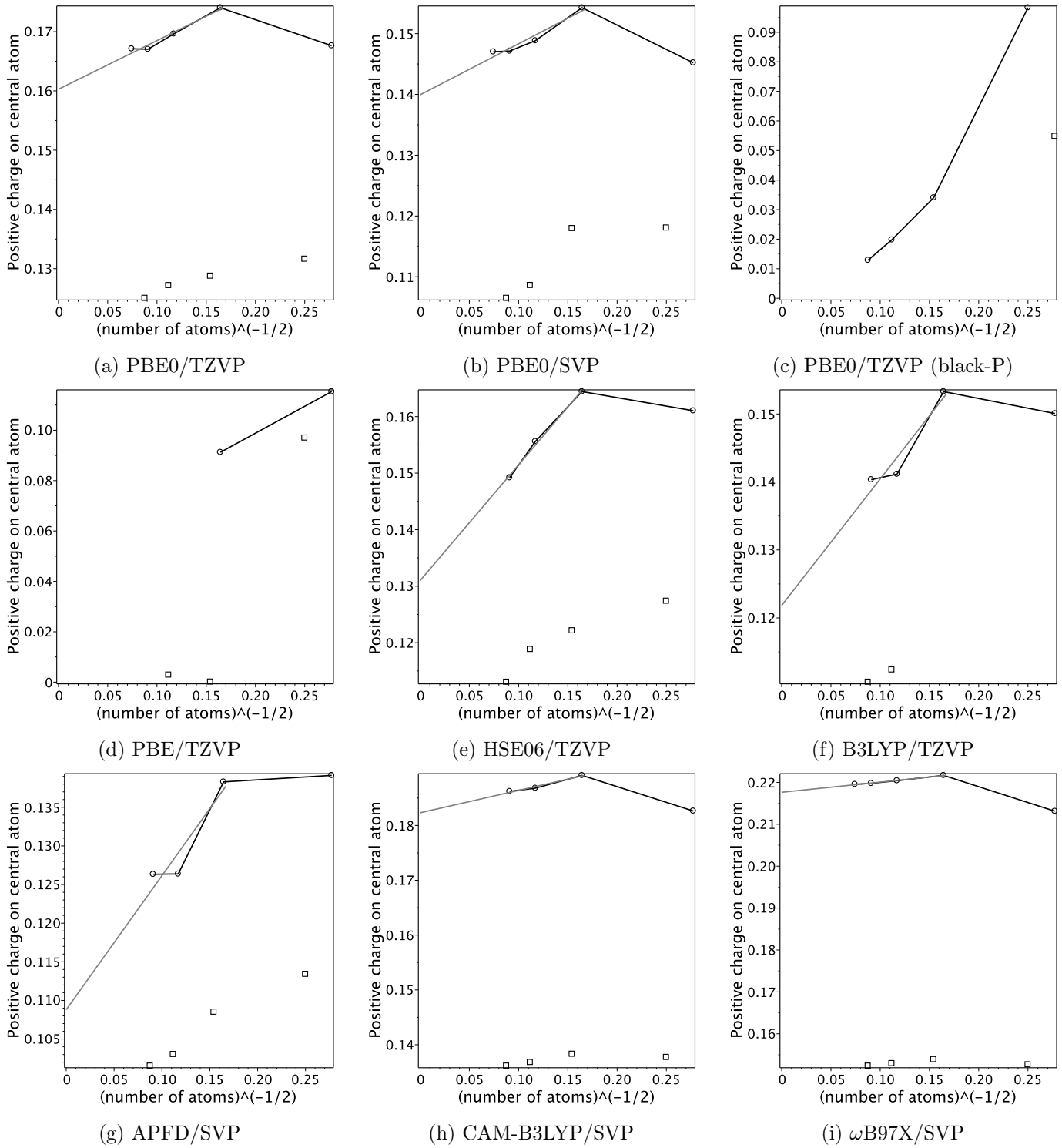

(a) PBE0/TZVP (b) PBE0/SVP (c) PBE0/TZVP (black-P)

(d) PBE/TZVP (e) HSE06/TZVP (f) B3LYP/TZVP

(g) APFD/SVP (h) CAM-B3LYP/SVP (i) ωB97X/SVP

Figure S27: Hole polaron extra charge on central atom for all considered density functionals for blue phosphorene clusters except for panel (c).

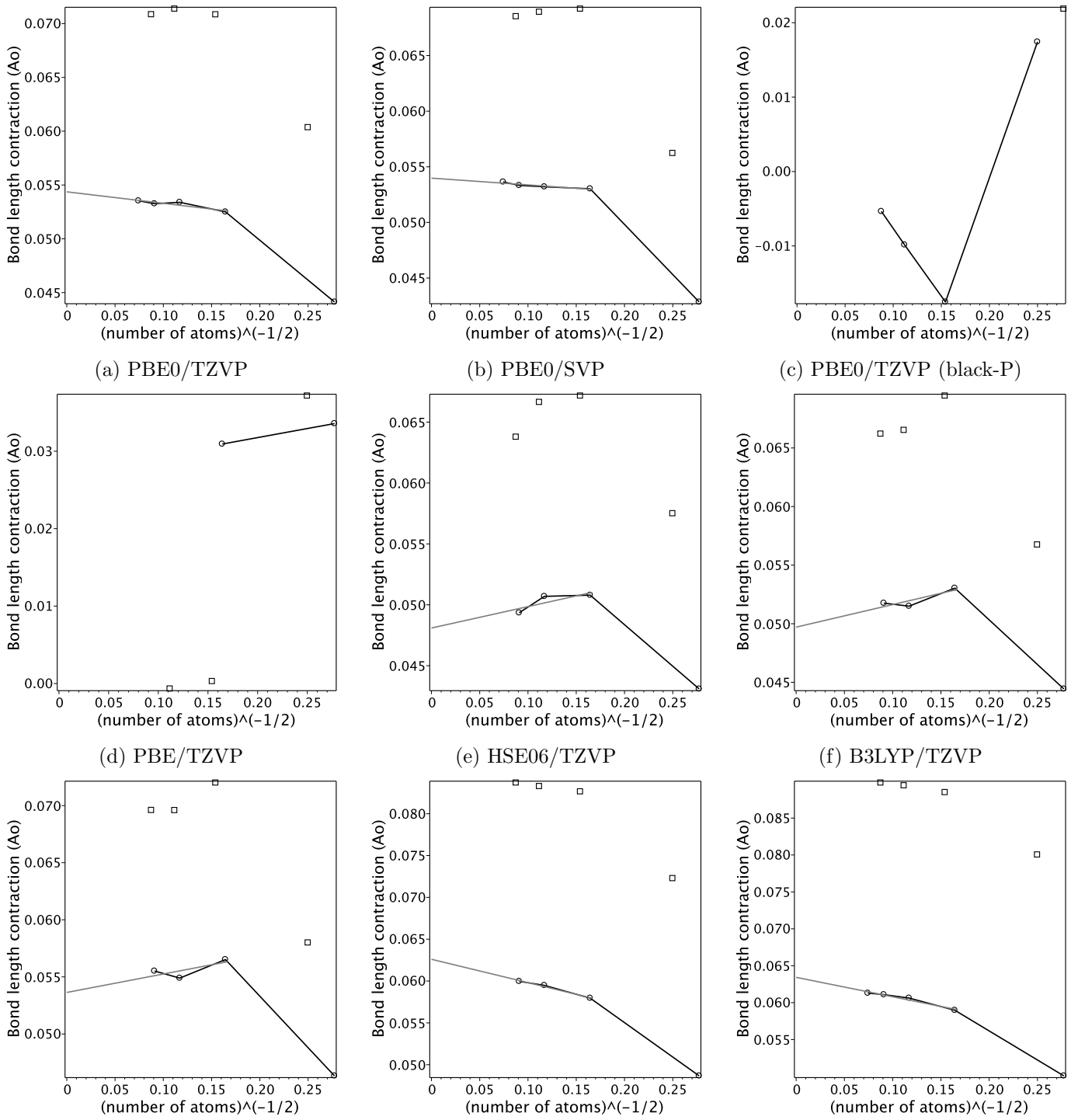

(a) PBE0/TZVP (b) PBE0/SVP (c) PBE0/TZVP (black-P)

(d) PBE/TZVP (e) HSE06/TZVP (f) B3LYP/TZVP

(g) APFD/SVP (h) CAM-B3LYP/SVP (i) ωB97X/SVP

Figure S28: Hole polaron central bond length contraction for all considered density functionals for blue phosphorene clusters except for panel (c).

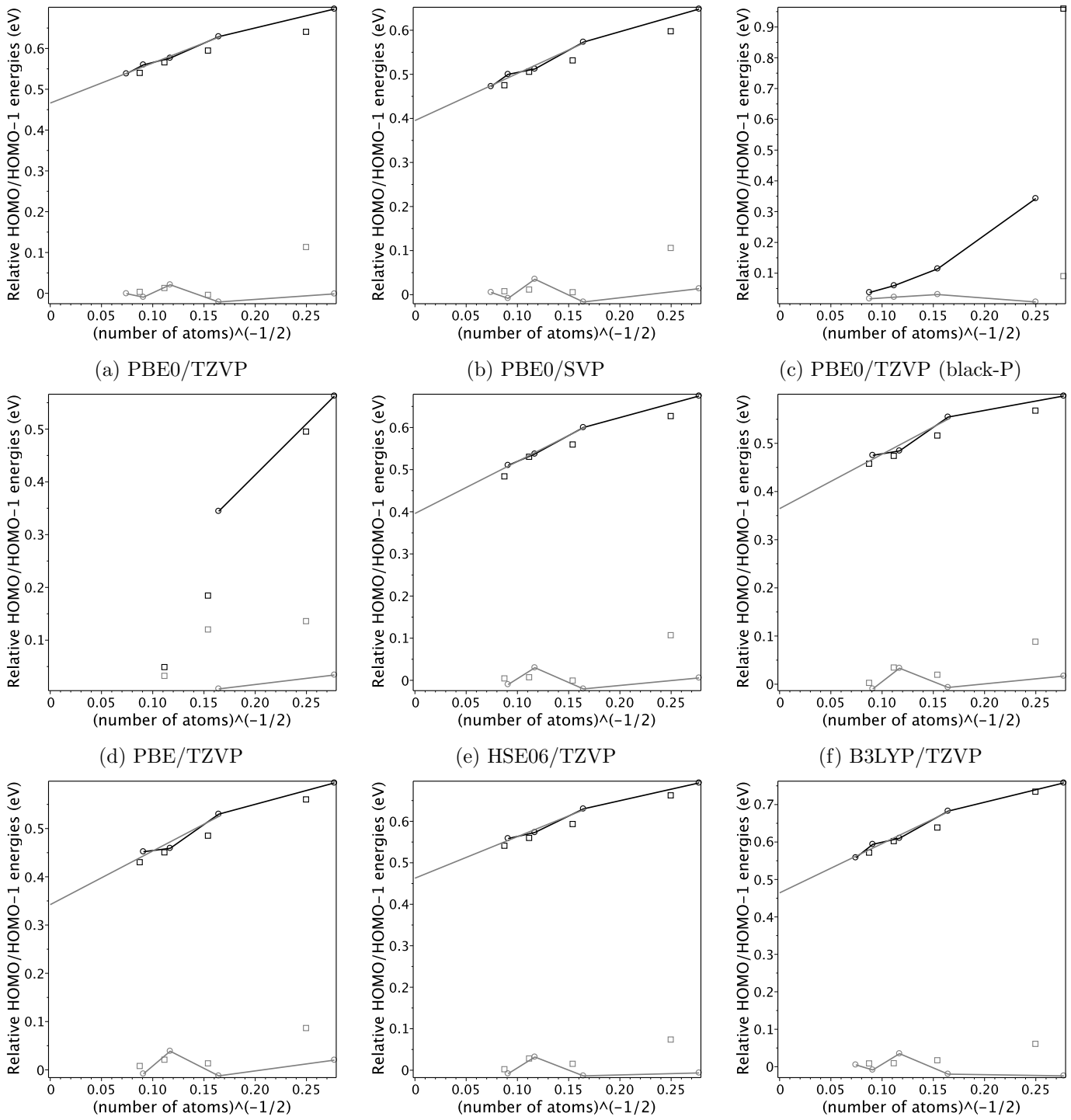

(a) PBE0/TZVP (b) PBE0/SVP (c) PBE0/TZVP (black-P)

(d) PBE/TZVP (e) HSE06/TZVP (f) B3LYP/TZVP

(g) APFD/SVP (h) CAM-B3LYP/SVP (i) ωB97X/SVP

Figure S29: Hole polaron localized electronic level for all considered density functionals for blue phosphorene clusters except for panel (c).

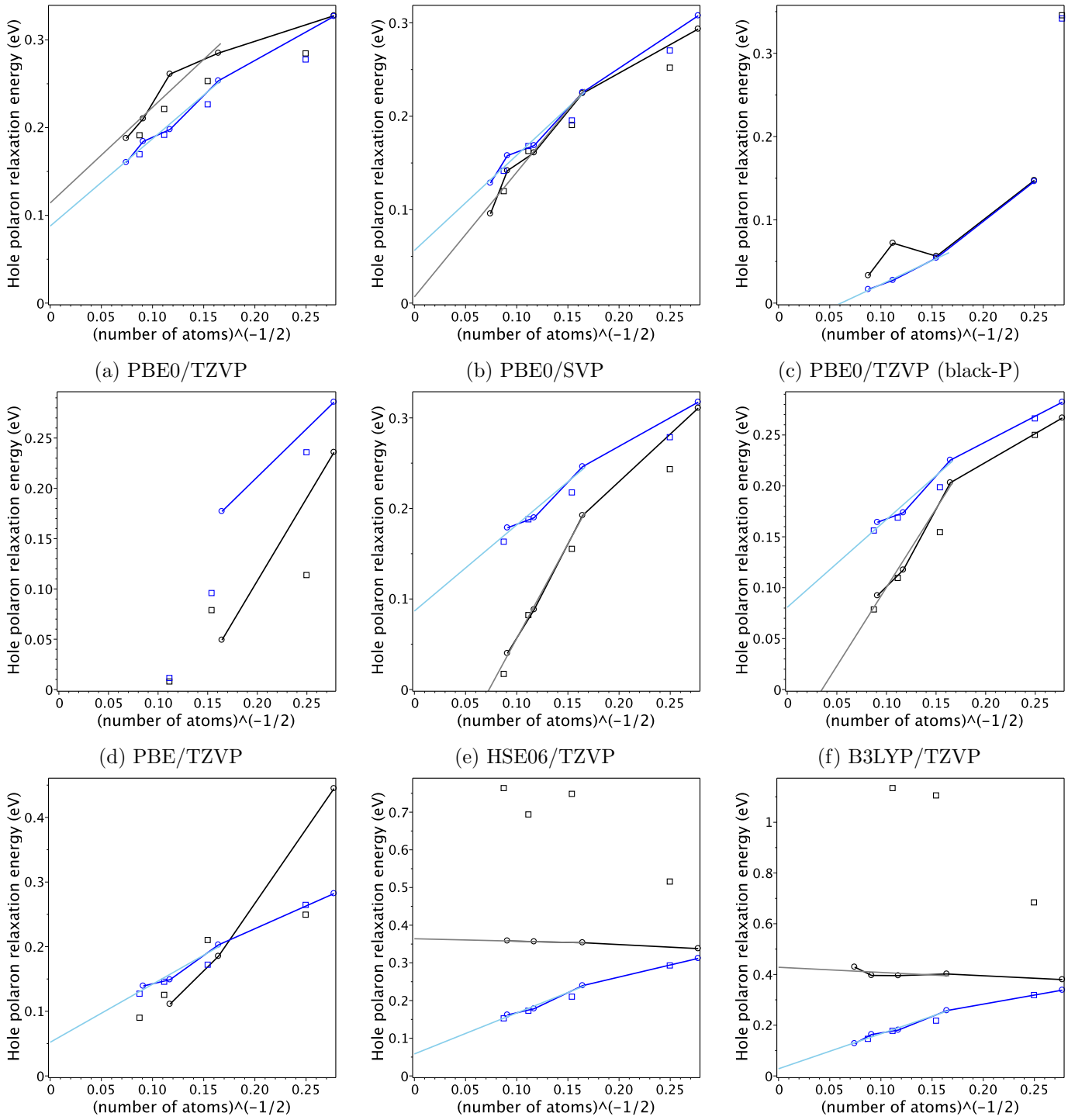

(a) PBE0/TZVP (b) PBE0/SVP (c) PBE0/TZVP (black-P)

(d) PBE/TZVP (e) HSE06/TZVP (f) B3LYP/TZVP

(g) APFD/SVP (h) CAM-B3LYP/SVP (i) ωB97X/SVP

Figure S30: Hole polaron relaxation energy calculated by Eq. 1 (black colored) and with approximation given by Eq. 2 (blue colored) for all considered density functionals for blue phosphorene clusters except for panel (c).

Table S7: Extrapolated parameters of the hole polaron in blue-P. Here Δq is the extra charge on central atom, Δd is the central bond length contraction (there are three such bonds), $\varepsilon^{\text{polaron}}$ is the polaron electronic level above the valence band edge, E^{polaron} is the polaron energy calculated with the use of Eq. 2, and $\Delta\text{IP}^{\text{v/a}} = \text{IP}^{\text{v/a}} + \varepsilon_{\text{HOMO}}$ where $\text{IP}^{\text{v/a}}$ is vertical/adiabatic ionization potential and HOMO is taken for relaxed neutral cluster.

Method	Δq	Δd	$\varepsilon^{\text{polaron}}$	E^{polaron}	$\Delta\text{IP}^{\text{v}}$	$\Delta\text{IP}^{\text{a}}$
	e	Å	meV	meV	meV	meV
PBE/TZVP					88	
APFD/SVP	0.109	0.0536	342	52	109	153
B3LYP/TZVP	0.122	0.0497	364	81	114	160
HSE06/TZVP	0.131	0.0481	396	87	45	342
PBE0/SVP	0.140	0.0540	395	56	112	95
PBE0/TZVP	0.160	0.0544	466	88	132	20
CAM-B3LYP/SVP	0.182	0.0626	463	58	-372	-739
WB97X/SVP	0.218	0.0634	464	28	-1048	-1484

S10 Potential energy surfaces

Computational methodology. In this work we use electron-phonon couplings defined through single-site Holstein Hamiltonian (independent boson model, displaced harmonic oscillator):

$$\mathsf{H} = \varepsilon \mathsf{n} + \sum_\alpha \hbar\omega_\alpha \left(\mathsf{b}_\alpha^\dagger \mathsf{b}_\alpha + \frac{1}{2} \right) + \sum_\alpha \hbar\omega_\alpha g_\alpha \left(\mathsf{b}_\alpha^\dagger + \mathsf{b}_\alpha \right) \mathsf{n}, \tag{S1}$$

where $\mathsf{n} = \mathsf{c}^\dagger \mathsf{c}$, $\mathsf{c}_i^\dagger$ is an electronic quasiparticle creation operator and $\mathsf{b}_\alpha^\dagger$ is phonon (vibrational normal mode) creation operator. Only a single electronic level ε is considered – it is the polaron level. A vibrational mode with frequency ω_α is coupled to the electronic level via dimensionless coupling constant g_α, so that $S_\alpha = g_\alpha^2$ is the corresponding Huang–Rhys factor. The polaron relaxation energy is given by

$$\Delta E_{\text{harmonic}}^{\text{charged}} = \sum_\alpha S_\alpha \hbar\omega_\alpha \equiv \sum_\alpha \lambda_\alpha = \frac{1}{\sqrt{2\pi\sigma^2}} \int \lambda(\omega)\, \mathrm{d}\omega, \tag{S2}$$

where the function

$$\lambda(\omega) = \sum_\alpha \lambda_\alpha \mathrm{e}^{-\left(\frac{\omega-\omega_\alpha}{\sigma}\right)^2} \tag{S3}$$

is plotted in Fig. 4c and σ is the line broadening parameter. The classical version of the above Hamiltonian is given by

$$\varepsilon \mathsf{n} + \frac{1}{2} \sum_\alpha \hbar\omega_\alpha \left(\omega_\alpha^{-2} \dot{\xi}_\alpha^2 + \xi_\alpha^2 \right) + \sqrt{2} \sum_\alpha \hbar\omega_\alpha g_\alpha \xi_\alpha \mathsf{n}, \tag{S4}$$

where ξ_α is the dimensionless vibrational coordinate. From this formula it is easy to obtain the relation between electron-phonon couplings and equilibrium displacements:

$$\xi_\alpha^{(0)} = -\sqrt{2} g_\alpha. \tag{S5}$$

In this way the couplings are computed from equilibrium geometries of the neutral and charged states using vibrational modes of the charged state.

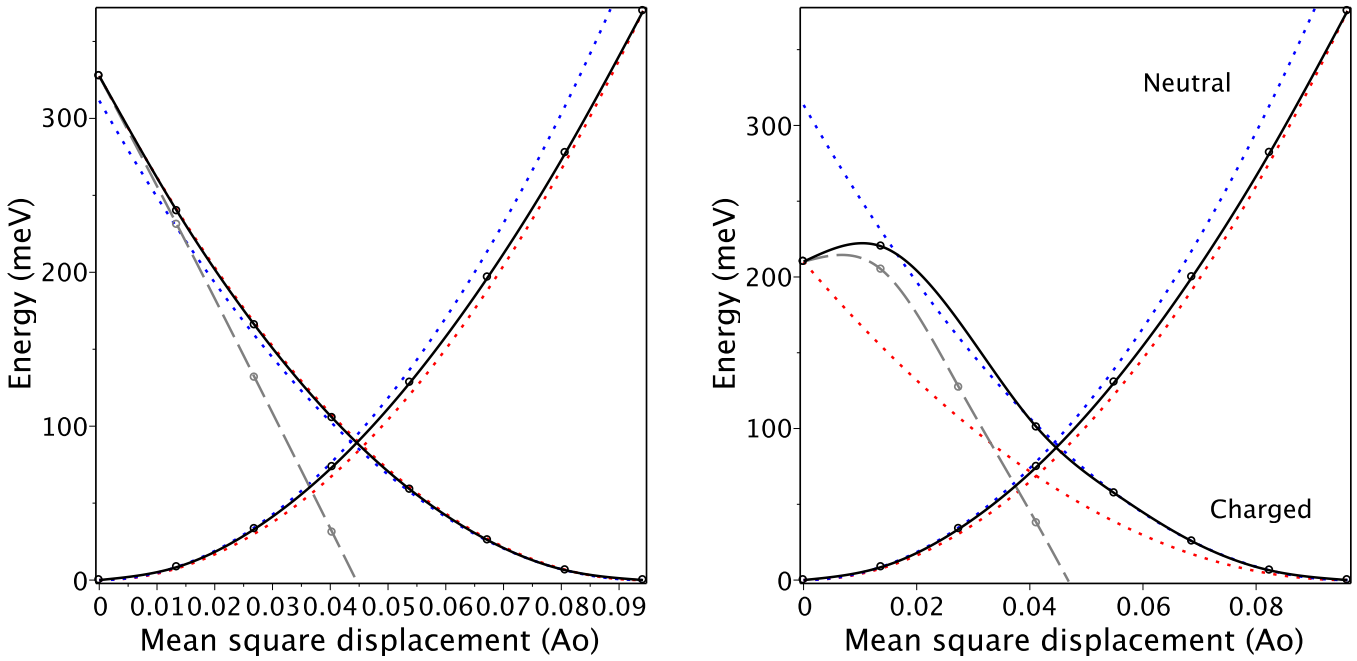

(a) (b)

Figure S31: Displacement potential energy surface for the blue-P cluster with (a) 13 and (b) 121 atoms. As the system size growths, there is a substantial deviation from the displaced harmonic oscillator: the asymmetry becomes larger and a qualitatively different state appears at zero displacement. Nevertheless the charged PES remains locally harmonic justifying use of linearized empirical Hamiltonians.

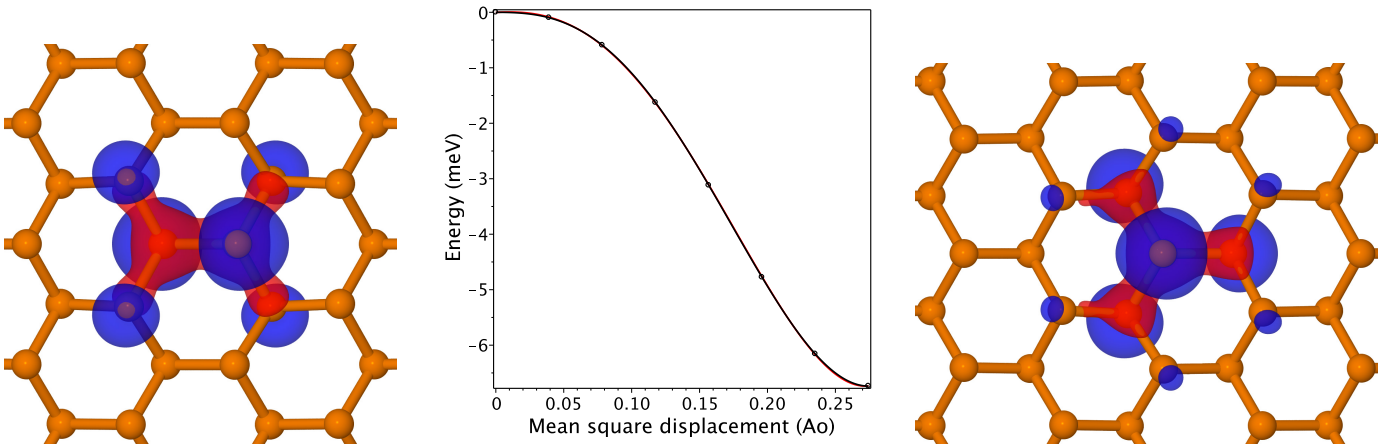

(a) (b) (c)

Figure S32: Adiabatic potential energy surface for polaron motion in blue-P: (a) polaron wave-function at saddle point between two minima; (b) linear PES scan between the saddle point and the minimum; (c) polaron wave-function at the minimum.

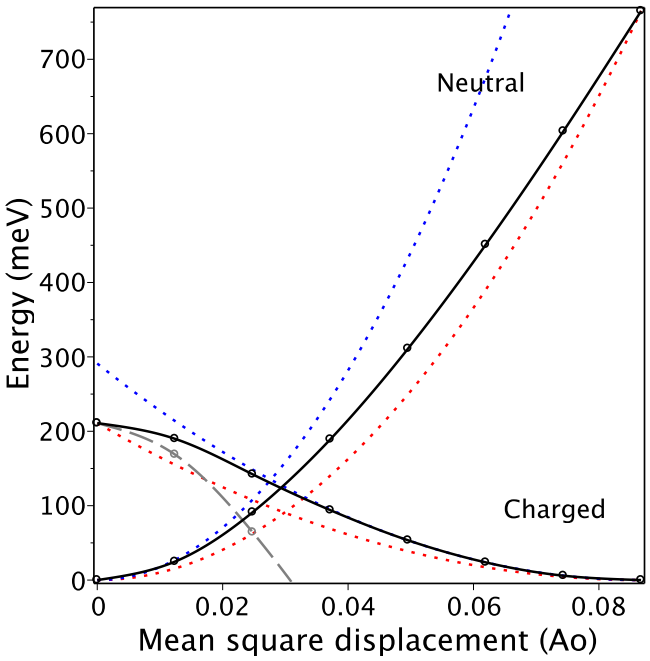

(a) Blue-P anion.

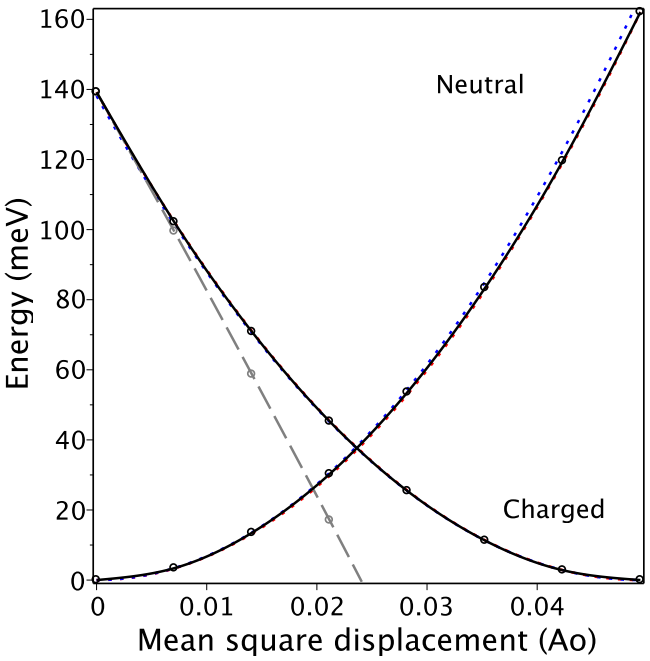

(b) Black-P anion.

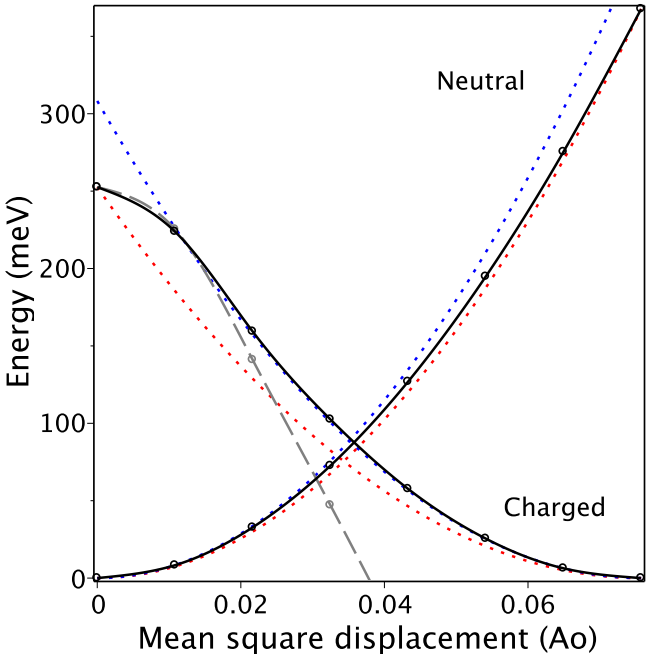

(c) Blue-P cation.

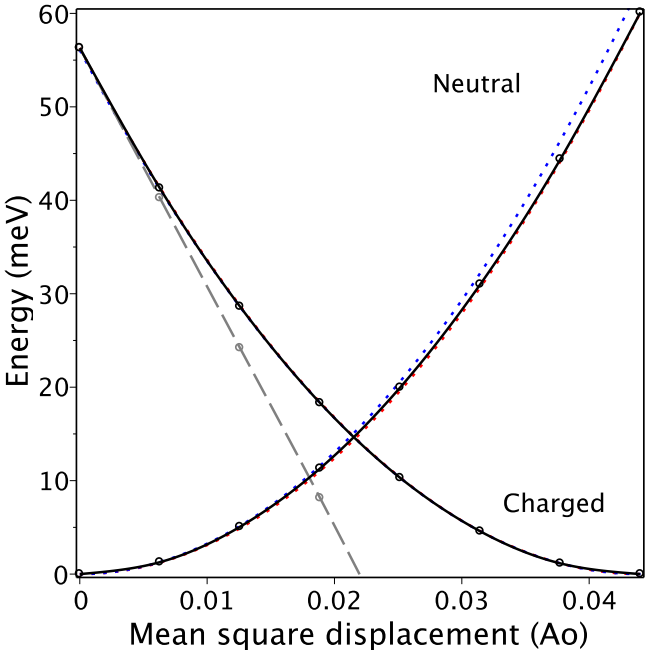

(d) Black-P cation.

Figure S33: Displacement potential energy surface for 42-atom clusters of the two allotropes and the two possible charges.

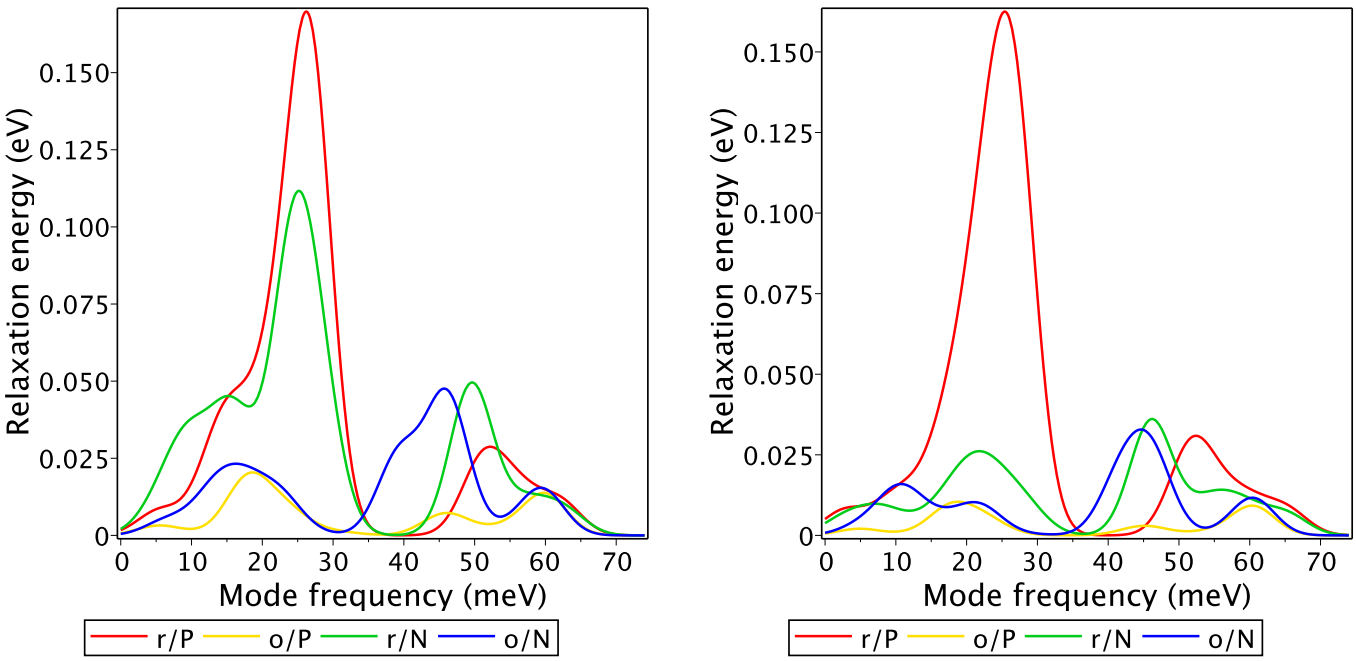

(a) 42-atom clusters.

(b) 80-atom clusters.

Figure S34: Spectral decomposition of the polaron harmonic relaxation energy $\Delta E^{\text{charged}}_{\text{harmonic}}$ for two cluster sizes of blue ('r') and black ('o') phosphorus cation ('P') and anion ('N').

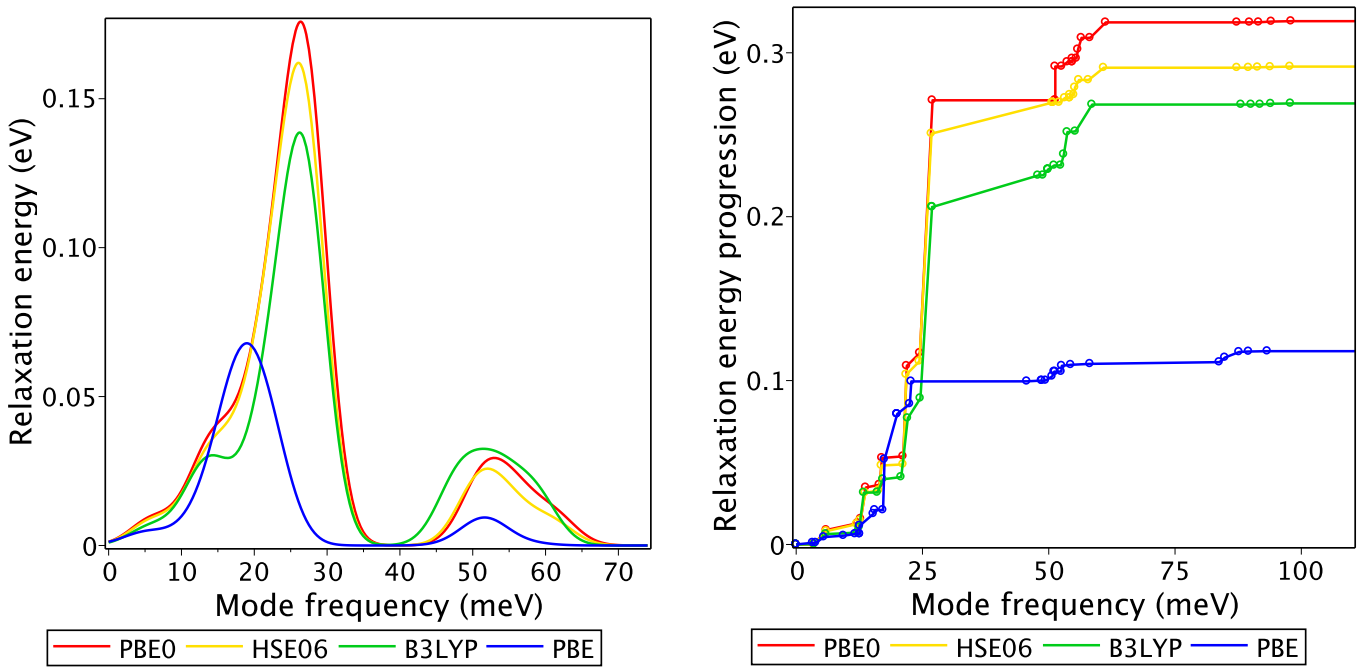

(a) (b)

Figure S35: Dependence of electron-phonon couplings on density functional for 37-atom blue-phosphorene cation.

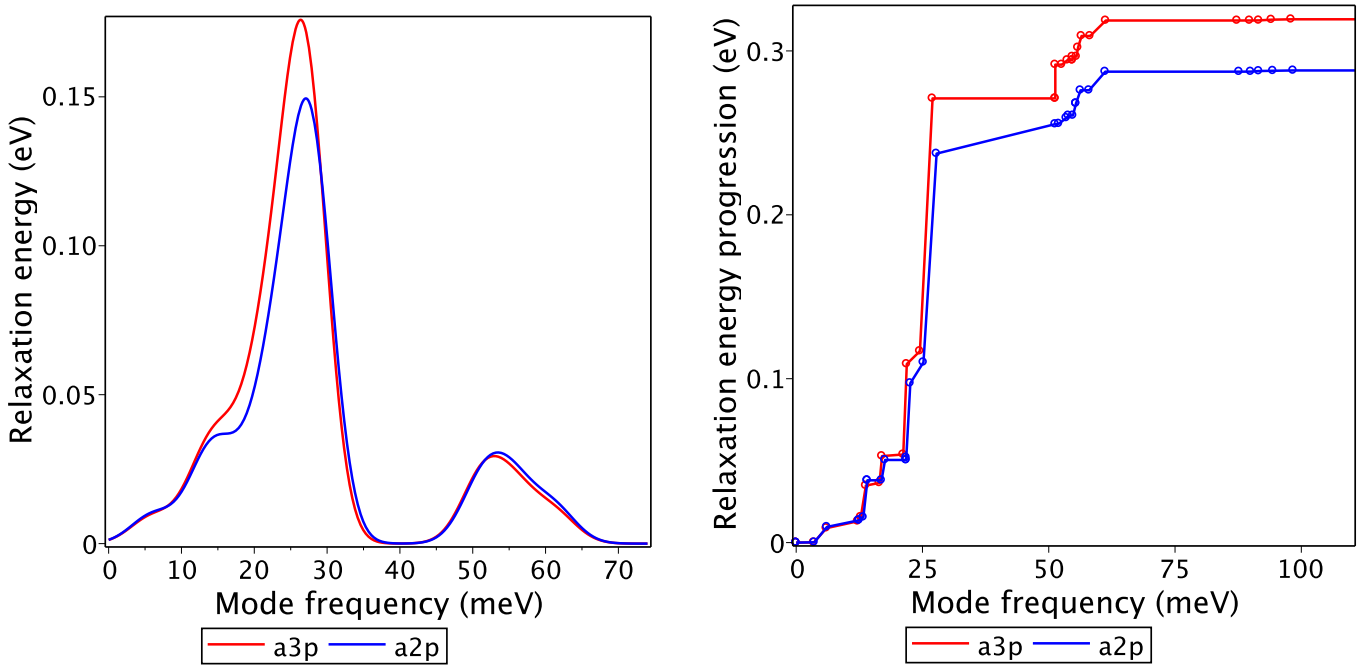

(a) (b)

Figure S36: Dependence of electron-phonon couplings on basis set for 37-atom blue-phosphorene cation. Here 'a3p'=TZVP, 'a2p'=SVP, and the density functional is PBE0.

S11 Excited states

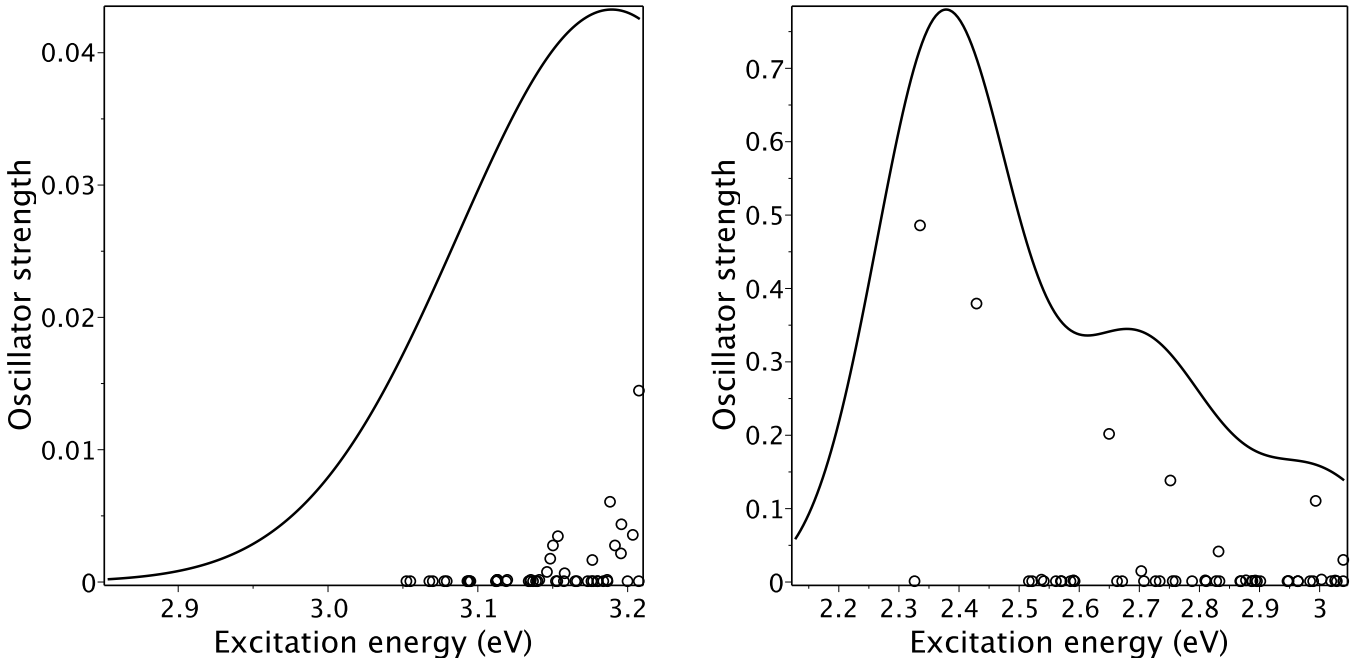

(a) Blue-P. (b) Black-P.

Figure S37: Gaussian-broadened (0.1 eV) oscillator strengths for 50 excited singlets of 130-atom clusters calculated by TDDFT (PBE0/TZVP).

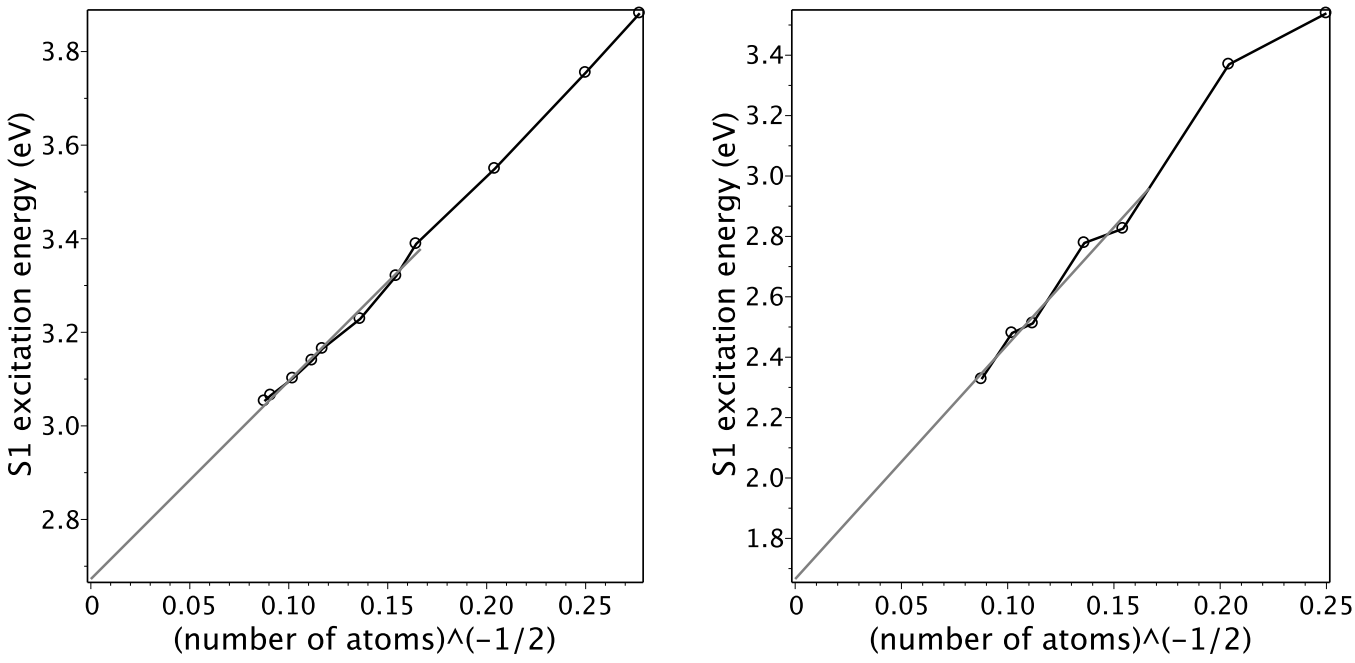

(a) Blue-P. (b) Black-P.

Figure S38: Size convergence of the lowest excited singlet energy (TDDFT, PBE0/TZVP).

S12 Triplet exciton

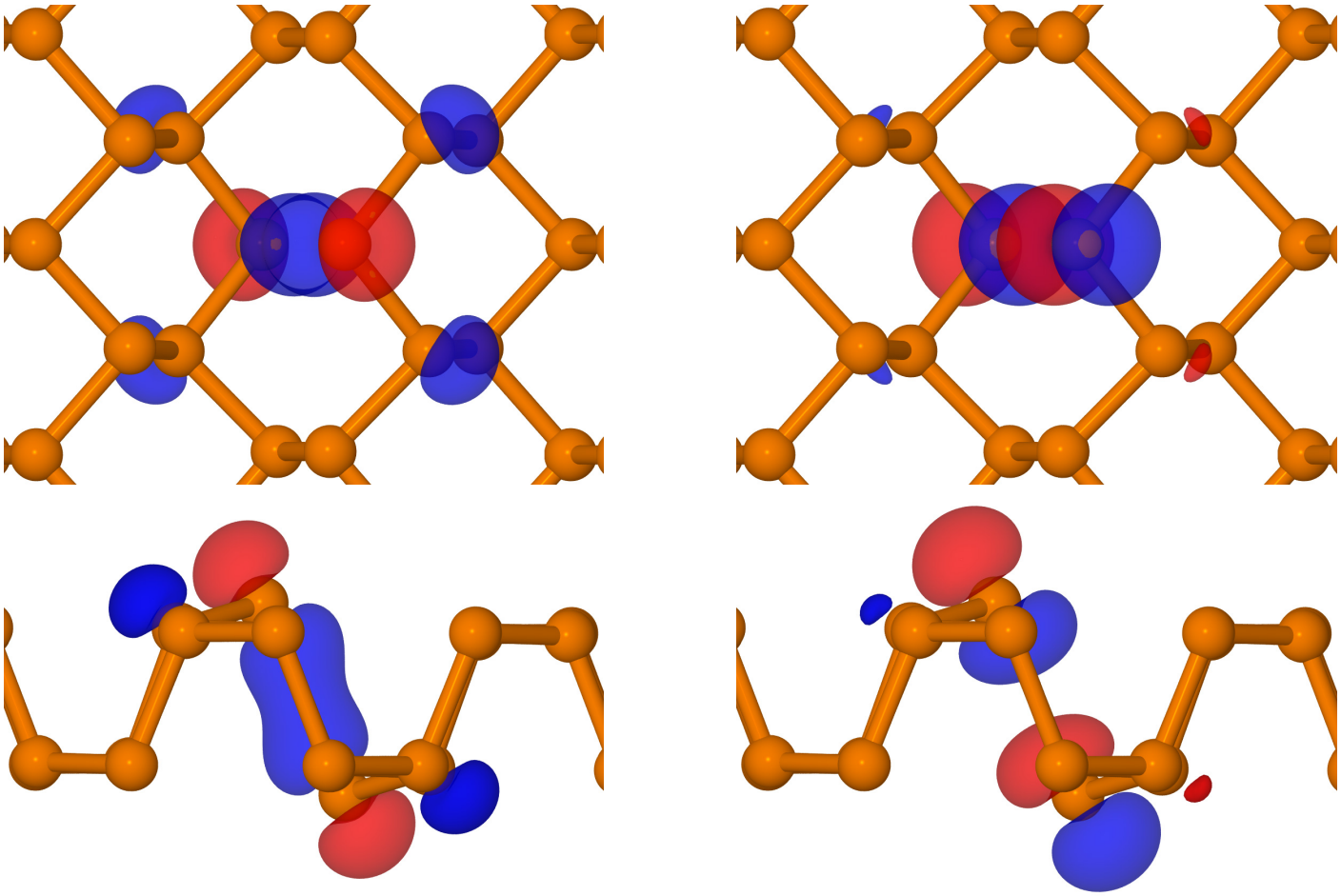

Figure S39: Unpaired natural orbitals of the triplet exciton in black-P.

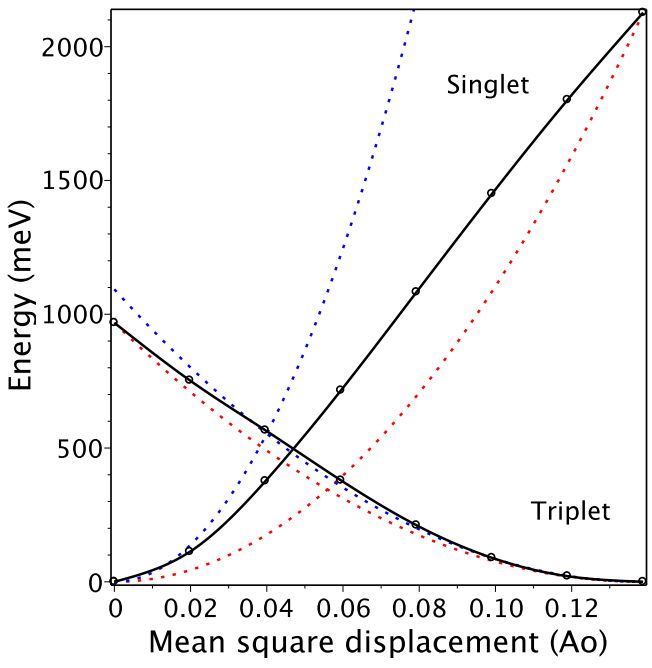

(a) Blue-P.

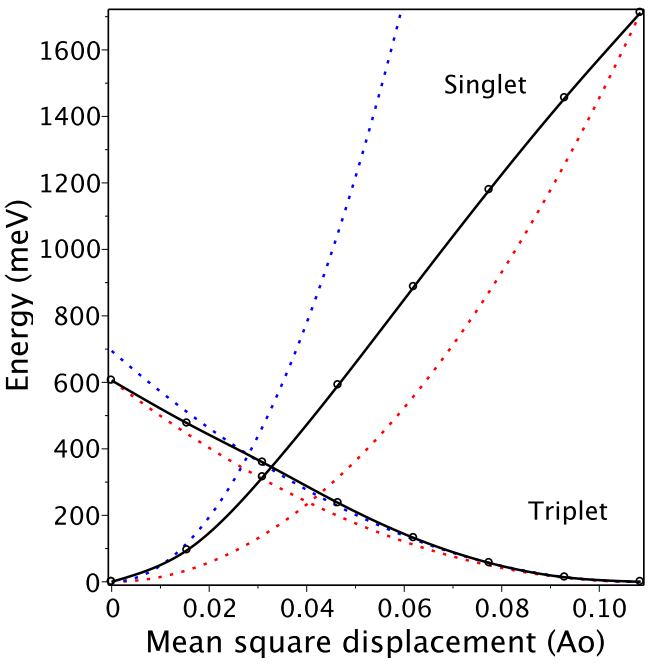

(b) Black-P.

Figure S40: Displacement potential energy surface for triplet exciton for 42-atom clusters of the two allotropes.

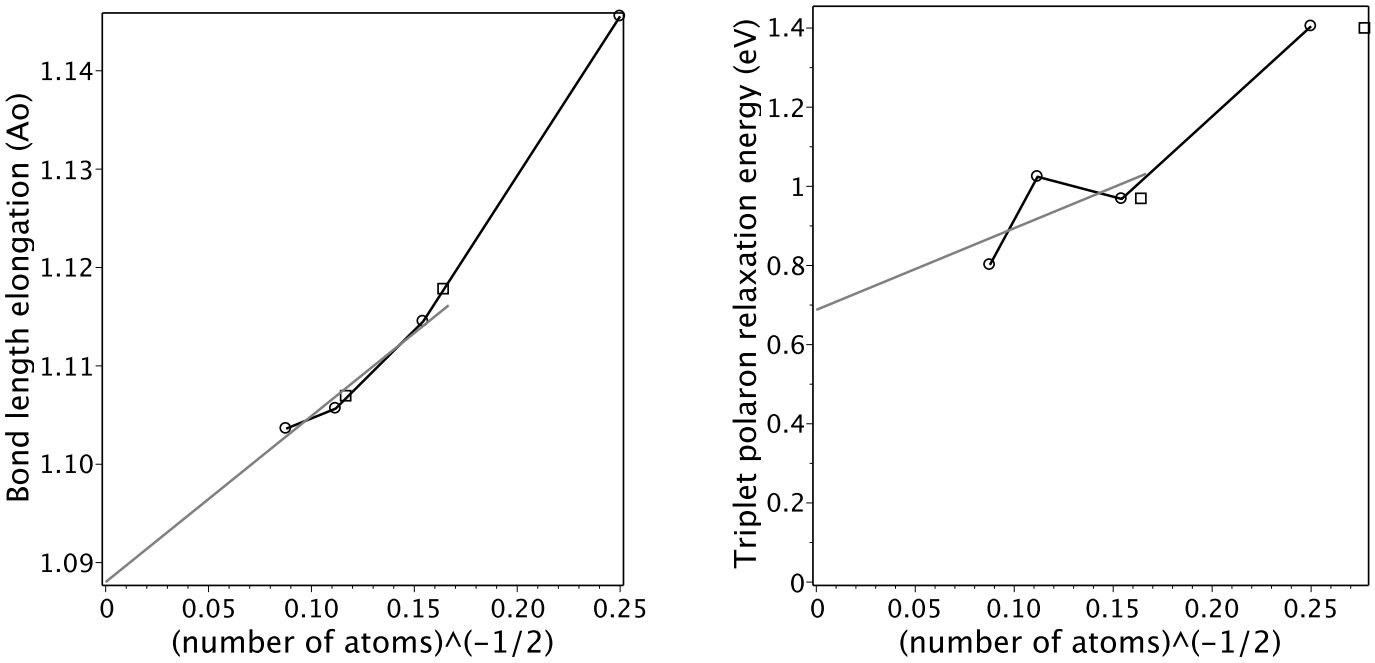

Figure S41: Cluster size convergence of the localized triplet exciton parameters in blue-P.

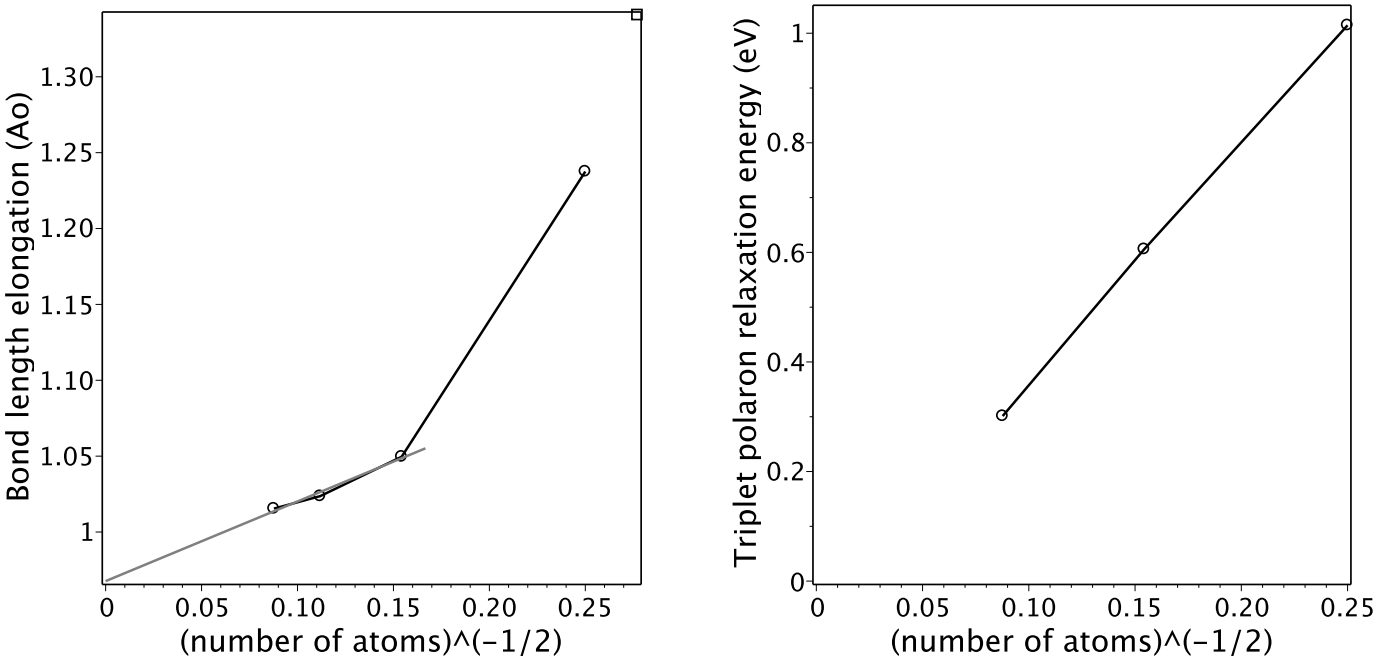

Figure S42: Cluster size convergence of the localized triplet exciton parameters in black-P.

S13 Results for arsenic

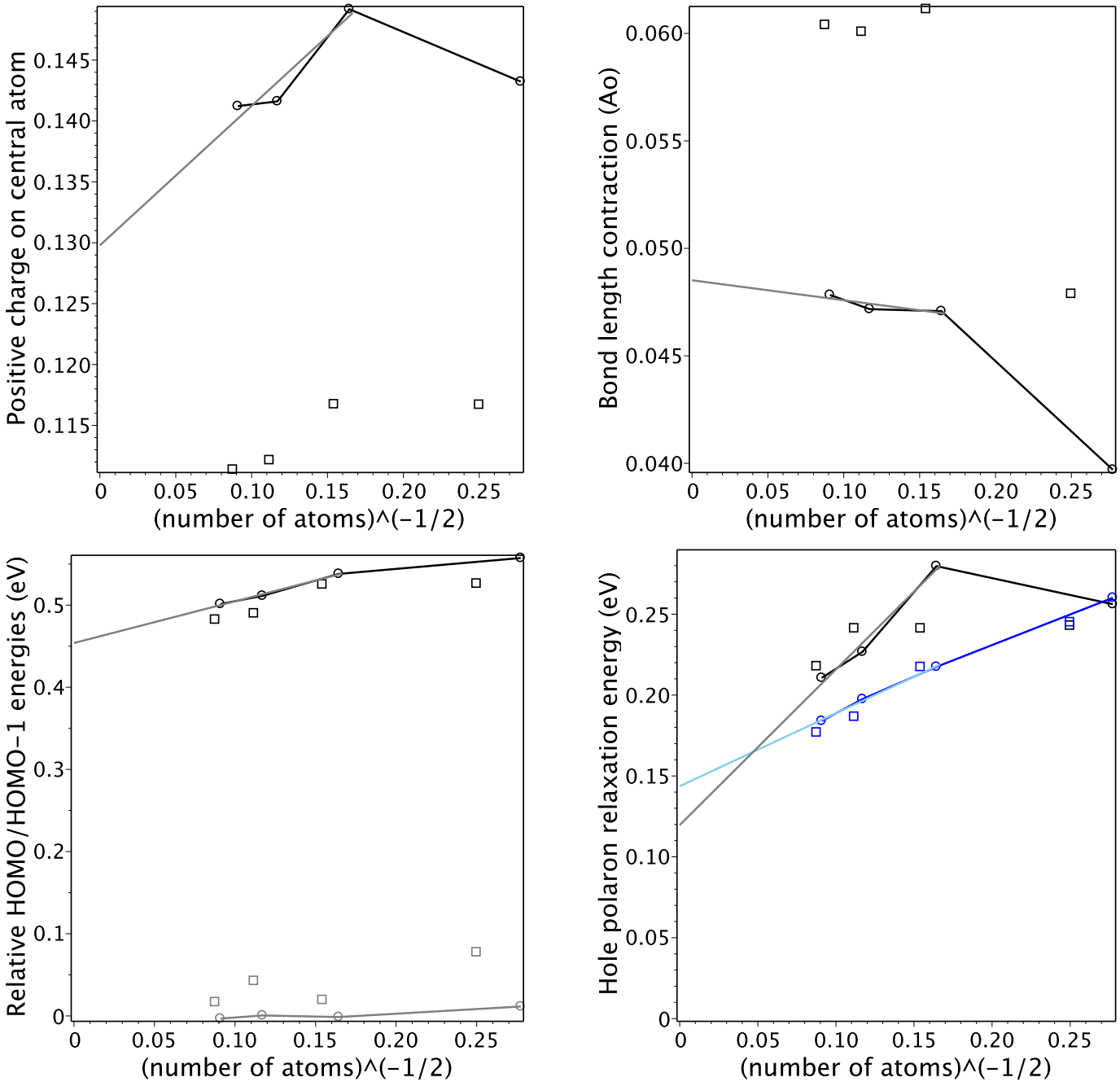

Figure S43: Cluster size convergence of the hole polaron parameters in blue-As (see Fig. 3 for explanation).

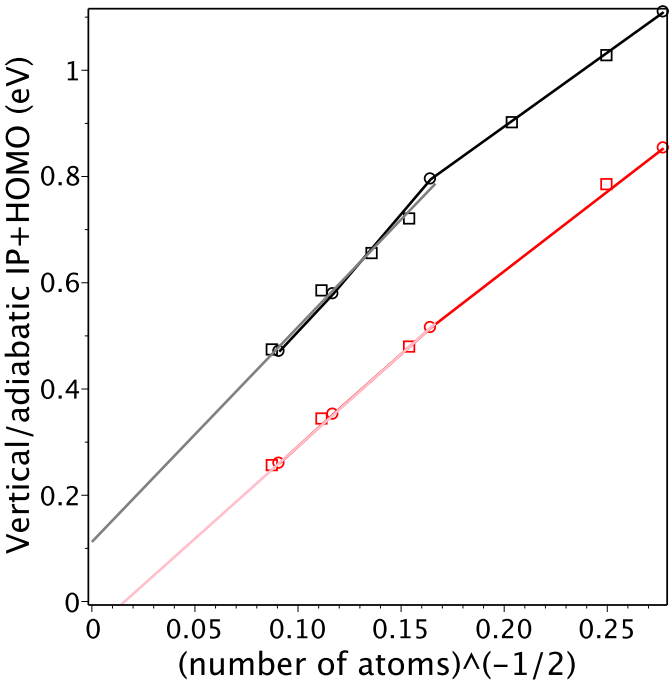

Figure S44: IP+HOMO for blue-As.

Table S8: Main parameters of blue- and black-As monolayers. See Table S5 for notations.

Method	dE	bondlengths		angles		gap	HOMO	LUMO	LP	bonding orbitals		
	meV	Ao	Ao	deg	deg	eV	eV	eV	eV	eV	eV	
--- paw400 ---												
PBE		2.509		92.0		1.60	-3.54	-1.93				
	37.2	2.496	2.511	94.5	100.6	0.81	-2.56	-1.76				*
--- a3p ---												
PBE		2.506		92.0		1.71	-5.48	-3.76				
	30.0	2.493	2.500	94.5	101.0	0.94	-4.76	-3.82				*
HSE06		2.479		92.3		2.40	-6.02	-3.63	-17.28	5.00		
	26.9	2.468	2.468	94.7	101.6	1.55	-5.19	-3.64	-16.30	3.60	3.62	*
B3LYP		2.511		93.2		2.93	-6.23	-3.30	-17.47	5.55		
	38.8	2.507	2.493	95.0	103.1	2.09	-5.42	-3.33	-16.56	4.39	4.27	*
PBE0		2.473		92.3		3.02	-6.34	-3.32	-17.55	4.79		
	29.0	2.461	2.461	94.6	101.7	2.21	-5.52	-3.31	-16.52	3.31	3.35	*
--- a2p ---												
PBE		2.512		91.8		1.79	-5.53	-3.75				
	27.8	2.501	2.509	94.7	100.5	0.93	-4.78	-3.85				*
HSE06		2.486		92.2		2.47	-6.11	-3.63				
	26.2	2.476	2.477	94.7	101.2	1.57	-5.28	-3.70				*
B3LYP		2.518		92.9		2.99	-6.24	-3.25	-17.04	5.54		
	39.0	2.513	2.502	94.9	102.6	2.12	-5.44	-3.32	-16.27	4.52	4.42	*
PBE0		2.481		92.1		3.11	-6.44	-3.34	-17.27	4.86		
	29.0	2.469	2.470	94.6	101.3	2.23	-5.63	-3.40	-16.38	3.52	3.53	*
WB97X		2.466		93.0		6.67	-8.32	-1.64				

S14 Results for antimony

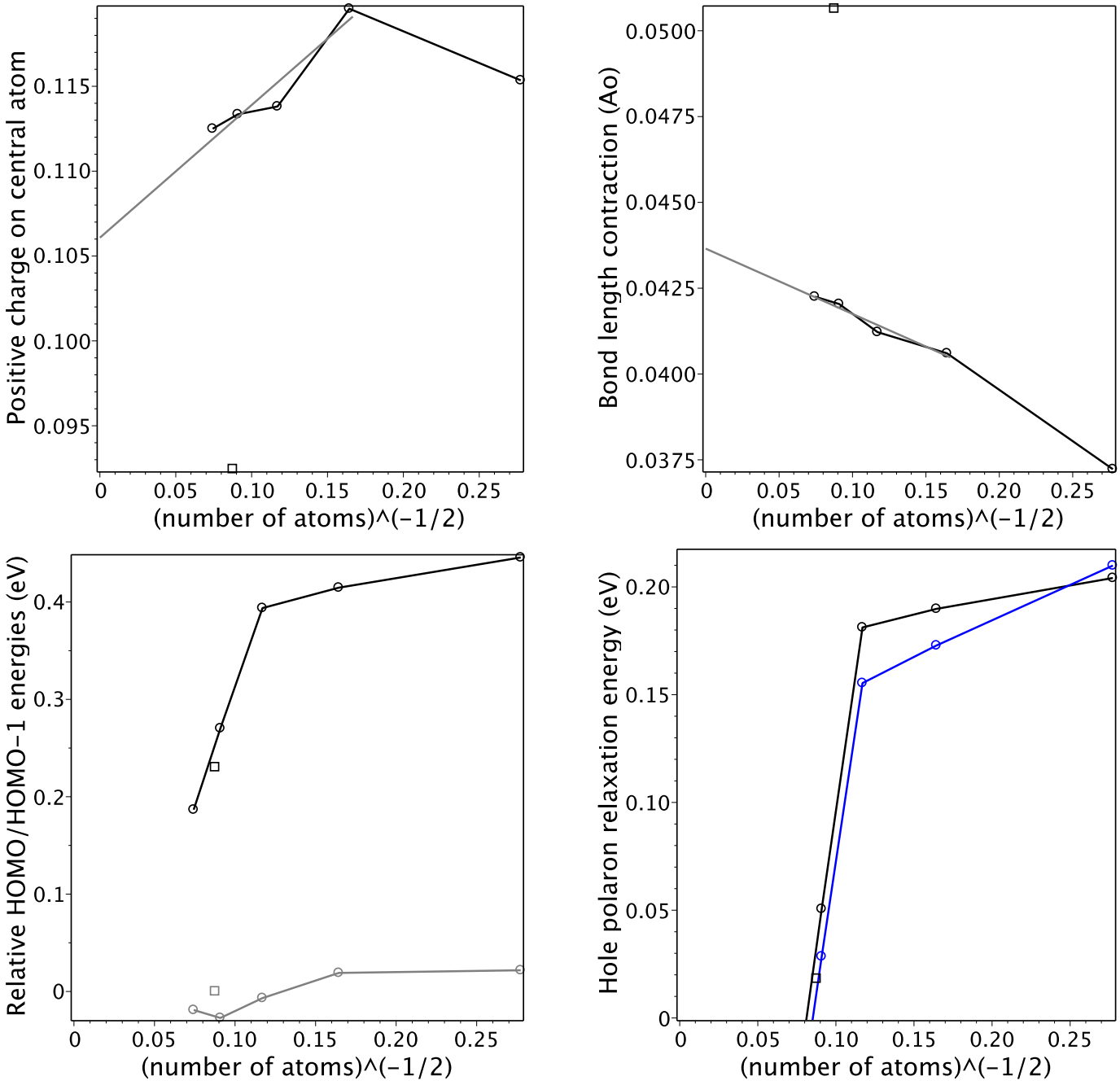

Figure S45: Cluster size convergence of the hole polaron parameters in blue-Sb (SVP basis, no spin-orbit coupling, see Fig. 3 for explanation).

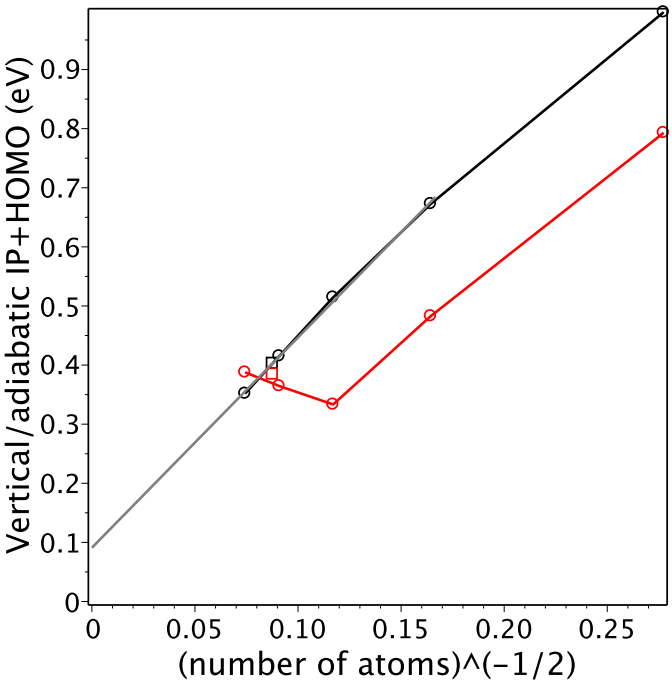

Figure S46: IP+HOMO for blue-Sb (SVP basis).

S15 Atomic data for pnictogens and related elements

Table S9: Atomic data for pnictogens, their cations and isoelectronic elements from NIST Atomic Spectra Database (DOI:10.18434/T4W30F). Shown here are level energies in eV relative to the ground state except for "spin-orbit" parameter. The latter is defined as the fine structure splitting between the listed level $^{2S+1}L_J$ and level $^{2S+1}L_{J-1}$. The "exchange" parameter involves energy difference between levels with the same electronic configuration but different spins, which is proportional to the exchange integral between p-orbitals. The rest of columns characterize relative energies of one-electron orbitals belonging to different shells and subshells: $s \to p$ is between valence orbitals and $p \to s, p, d$ is between the valence and the next shell. In all these cases the lowest energy excitation is listed; if its symmetry is different from the one indicated in the heading row, the symmetry is listed right to the energy. Multiconfigurational states are combined (the top last column). For heavy elements (Bi and Pb) jj-coupling scheme is used and thus level re-interpretation in LS-coupling is not always obvious.

s^2p^3 elements, ground state is $^4S^o_{3/2}$								
	spin-orbit	exchange		$p \to s$	$p \to p$		$s \to p, p \to d, s$	
	$^2D^o_{5/2}$	$^2D^o_{3/2}$		$^4P_{1/2}$	$^2S^o_{1/2}$		$^4P_{5/2}$	
N	.001	2.38		10.33	11.60		10.92	
P	.002	1.41		6.94	7.96		7.38	
As	.040	1.31		6.29	7.46		6.86	
Sb	.17	1.06		5.36	6.41		6.63	
Bi	.50	1.42		4.04	5.10		5.44	–
s^2p^2 elements and ions, ground state is $^3P_0$								
	spin-orbit	exchange	$s \to p$	$p \to s$	$p \to p$		$p \to d$	
	$^3P_1$	$^1D_2$	$^5S^o_2$	$^3P^o_0$	$^1P_1$		$^1D^o_2$	
C	.002	1.26	4.18	7.48	8.54		–	
Si	.010	0.78	4.13	4.92	5.86		5.87	
Ge	.069	0.88	5.20	4.64	5.70	$^3D_1$	6.01	
Sn	.21	1.07	4.91	4.29	5.25	$^3D_1$	5.42	$^3F^o_2$
Pb	.97	2.66	–	4.33	5.32	–	5.63	–
N^+	.006	1.90	5.80	18.46	20.41		–	
P^+	.020	1.10	5.67	10.74	12.60		9.63	
As^+	.13	1.25	6.80	9.76	11.82	?	10.30	
Sb^+	.38	1.59	6.41	8.57	10.39	$^3D_1$	8.98	
Bi^+	1.65	4.21	9.44	8.57	10.45	–	9.81	–

S16 Dependence on cluster passivation

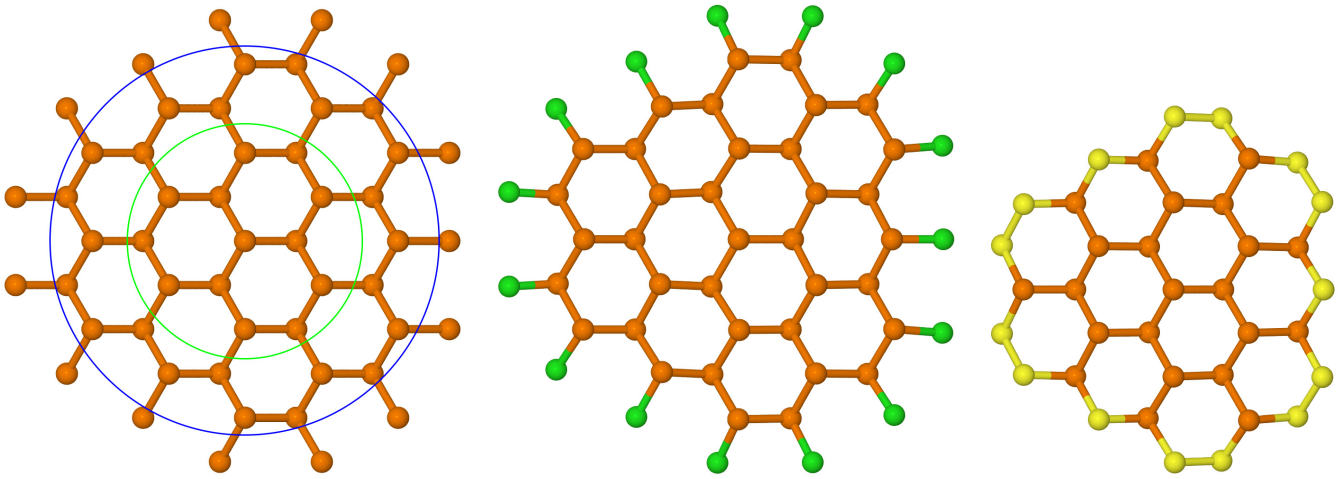

(a) ONIOM calculations (b) Chlorine-passivated cluster (c) Sulfur-passivated cluster

Figure S47: Other passivations considered. The ONIOM calculations are performed with the standard settings of Gaussian 16 program; the molecular mechanics layer includes atoms beyond the blue circle; positions of atoms beyond the green circle are fixed in the infinite monolayer geometry. Note that the interior of sulfur-passivated clusters is compressed because S-S and S-P bonds are shorter than P-P bonds.

Table S10: Dependence of hole polaron relaxation energy on cluster passivation for blue-P. "Charge" is the NAO charge of the central atom. For the largest considered Cl-passivated cluster the wave-function of the undistorted cation has not been converged.

	Cluster size				
	37	73	121	181	
Passivation	Energies (meV)				Charge
H	224	161	142	96	-0.0014
ONIOM	232	168	151	105	-0.0015
Cl	257	206	150	—	+0.0007
S	79	92	104	116	+0.0206

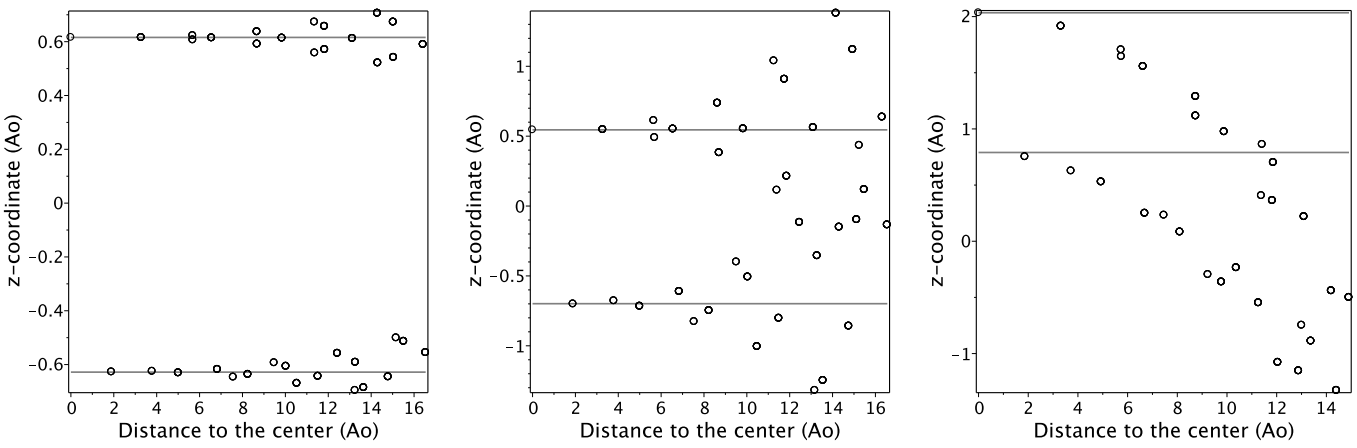

(a) Hydrogen-passivated cluster (b) Chlorine-passivated cluster (c) Sulfur-passivated cluster

Figure S48: Geometry of the considered clusters (181 atoms): z-coordinate of phosphorus atoms in the orientation of Fig. 1. The gray colored lines show z-coorinates of the infinite monolayer.